SAPIENZA
UNIVERSITÀ DI ROMA

**SCHOOL OF BIOLOGY AND MOLECULAR MEDICINE**

**PhD in IMMUNOLOGICAL SCIENCES**
**CYCLE XXIV**

# *"Transient Receptor Potential Vanilloid 1 (TRPV1) activation induces autophagy in thymocytes through ROS-regulated AMPK and Atg4C pathways"*

**Coordinator: Prof. Angela Santoni** **Tutor: Prof. Giorgio Santoni**

**Candidate: Valerio Farfariello**

***- Academic Year 2010/2011 -***

# Summary

# 1. INTRODUCTION

## 1.1 AUTOPHAGY: AN OVERVIEW

The word “autophagy” derives from Greek and means to eat (“phagy”) oneself (“auto”). This process is not directly a death pathway, rather a self-cannibalization pathway. Mainly mediated via the lysosomal degradation way, autophagy is responsible for degrading cellular proteins and is currently the only known process for degrading cellular organelles, recycling them to ensure cell survival. Thus autophagy, is one of the main mechanisms for maintaining cellular homeostasis. Nevertheless, in the recent years autophagy has been shown to engage in a complex interplay with apoptosis. In some cellular settings, it can serve as a cell survival pathway, suppressing apoptosis, and in others, it can lead to death itself, either in collaboration with apoptosis or as a back-up mechanism when the former is defective.

The term autophagy can be addressed to three different processes, depicted in Fig. 1: chaperone-mediated autophagy, microautophagy and macroautophagy. Chaperone-mediated autophagy (CMA) is characterised by its selectivity regarding the specific substrates (cytosolic proteins) degraded and involves direct translocation of unfolded substrate proteins across the lysosome membrane through the action of a cytosolic and

lysosomal chaperone hsc70, and the integral membrane receptor LAMP-2A (lysosome-associated membrane protein type 2A).

Microautophagy and macroautophagy, with respect to CMA, involve dynamic rearrangement of the sequestering membrane. The main difference between these two modes lies in the way by which cytoplasmic material is delivered to the lysosome but share in common the final steps of lysosomal degradation with eventual recycling of the degraded material. Microautophagy involves the engulfment of cytoplasm directly at the lysosomal surface, by invagination, protusion, and/or septation of the lysosomal limiting membrane. In contrast, macroautophagy involves the formation of cytosolic double-membrane vesicles that sequester portions of the cytoplasm. Fusion of the completed vesicle, an autophagosome, with the lysosome results in the delivery of an inner vesicle or autophagic body into the lumen of the degradative compartment [1].

In the present work, as for the scientific community, the term autophagy will refer to macroautophagy.

At present, more than 30 autophagy-related (Atg) genes and proteins have been identified in yeast and many of these have mammalian orthologs.

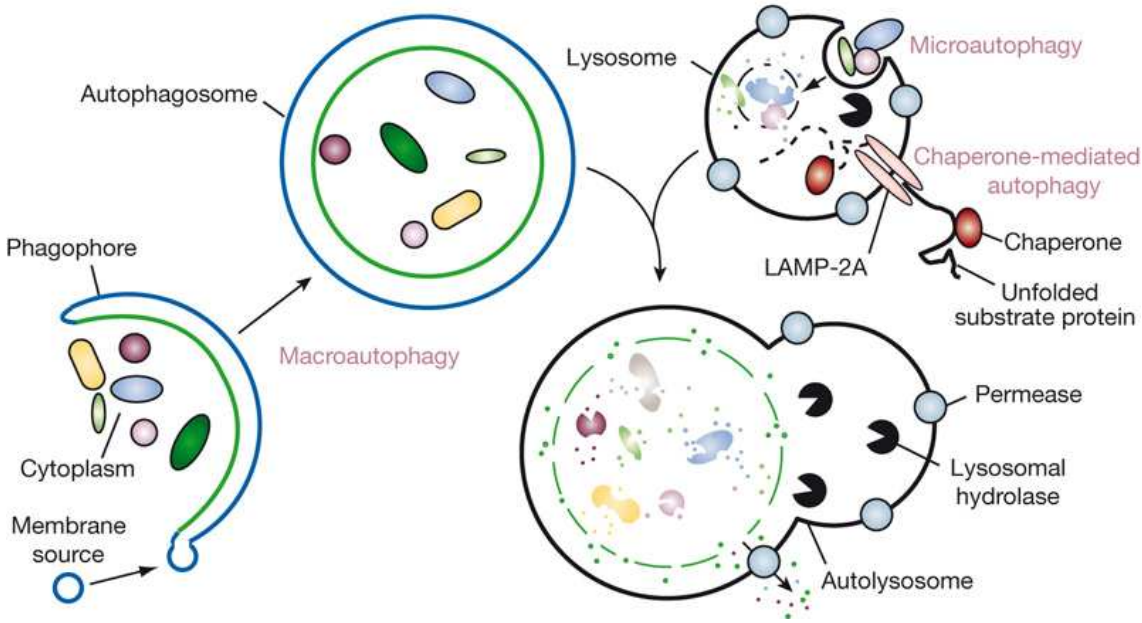


**Fig. 1**
Microautophagy refers to the sequestration of cytosolic components directly by lysosomes through invaginations in their limiting membrane. The function of this process in higher eukaryotes is not known, whereas microautophagy-like processes in fungi are involved in selective organelle degradation. In the case of macroautophagy, the cargoes are sequestered within a unique double-membrane cytosolic vesicle, an autophagosome. Sequestration can be either nonspecific, involving the engulfment of bulk cytoplasm, or selective, targeting specific cargoes such as organelles or invasive microbes. The autophagosome is formed by expansion of the phagophore, but the origin of the membrane is unknown. Fusion of the autophagosome with an endosome (not shown) or a lysosome provides hydrolases. Lysis of the autophagosome inner membrane and breakdown of the contents occurs in the autolysosome, and the resulting macromolecules are released back into the cytosol through membrane permeases. CMA involves direct translocation of unfolded substrate proteins across the lysosome membrane through the action of a cytosolic and lysosomal chaperone hsc70, and the integral membrane receptor LAMP-2A (lysosome-associated membrane protein type 2A). [2]

The autophagic process can be dissected into distinct steps :

***- Induction -***

The degradative autophagy pathway is induced upon starvation or different signaling pathways through a mechanism that involves the protein kinase Tor, a negative regulator of autophagy [3]. Tor can inhibit autophagy by two mechanisms [4]:

- acting in a signal transduction cascade through downstream effectors for the control of translation and transcription

- lowering the affinity of Atg13 for Atg1 by hyperphosphorylating Atg13 and thus inhibiting autophagy [5].

Atg1 and Atg13 are presumed to be part of a complex but most of the other components are still unknown. Both the regulatory kinases, Tor and the amino acid sensor general control nonrepressed 2 (Gcn2), and the Atg1 component of the induction complex play a conserved role in autophagy in higher eukaryotes [4, 6, 7].

***- Cargo Selection and Packaging –***

In *S. cerevisiae*, many of the components of the autophagic machinery are used for a specific transport called the cytoplasm to vacuole targeting (Cvt) pathway [8]. By this way, autophagy becomes a specific process through utilization of additional components, like Atg11 and Atg19 proteins, that are involved in the recognition and packaging of cargo. However, this

selectivity seems to be lost in higher eukaryotes and there is no evidence for the Cvt pathway in any organism other than *S. cerevisiae*.

***- Vesicle Nucleation -***

This step is not completely understood but the site of vesicle formation seems to be identified as the preautophagosomal structure PAS [9, 10]. Autophagic vesicles do not appear to bud off from preexisting organelles, as for vesicle formation throughout the endomembrane system of endoplasmic reticulum or Golgi complex. Thus, the vesicle is thought to form de novo but the source of the vesicle membrane is still unknown.

The most common hypothesis is that the endoplasmic reticulum supplies membrane during vesicle formation, although the mechanism by which a portion of the endoplasmic reticulum is switched from its normal function into esicle formation is not clear [11]. However, vesicle nucleation is tightly regulated by the phosphatidylinositol (PtdIns) 3-kinase complex I, which includes the PtdIns 3-kinase Vps34, along with Vps15, Vps30/Atg6, and Atg14 [12]. The transmembrane protein Atg9 also appears to act early in the process of vesicle formation. Atg9, Vps15, Vps34, and Vps30/Atg6 (Beclin 1) are conserved in higher eukaryotes.

***- Vesicle Expansion and Completion -***

The step of vesicle formation involves a lot of proteins that are either conjugating enzymes or structural. In the first group are two sets of components involving ubiquitin-like (Ubl) proteins that participate in

conjugation reactions during vesicle expansion [13]. Atg8 (LC3) is a Ubl that undergoes proteolytic processing prior to modify the lipid phosphatidyl-ethanolamine. Atg12, a second Ubl, is covalently attached to Atg5. One of the major questions concerning sequestering vesicle formation is what supplies the driving force for deformation/curvature of the membrane. In most vesicle budding processes, a central role is played by protein components that form a transient coat. The Atg12-Atg5 proteins are the best candidates for a transient coat complex involved in autophagy. Interestingly, almost all of the components that act at this stage of the pathway have orthologs in at least some higher eukaryotes [14].

***- Vesicle Targeting, Docking, and Fusion -***

During this phase, the autophagosome fuses with the lysosome, as a result the contents of the autophagosome are released into the lysosome for degradation by lysosomal proteases Molecular genetic studies have indicated that the machinery required for the fusion of autophagosomes vesicles with the vacuole includes the SNARE proteins GDI homologs and members of the class C Vps/HOPS complex [15].

***- Vesicle Breakdown -***

Following fusion of these two vesicle bodies, the autophagosome membrane is then broken down by the lysosomal protease (such as proteinase B) and the acidic pH of the vacuole lumen. From now on, the degraded content is ready to be recycled [1].

## 1.2 AUTOPHAGY AND IMMUNITY

There are growing evidence that autophagy is involved in the regulation of the immune system. This pathway has been linked both to innate and adaptive immunity, including pathogen resistance, production of type I interferon, antigen presentation, tolerance and lymphocyte development, as well as the negative regulation of cytokine signaling and inflammation.

Autophagy genes are involved in antimicrobial host defense in mammals, as demonstrated by phagocytic cell–specific deletion of Atg5 in mice that results in greater susceptibility to infection with two different types of intracellular pathogens, the bacterium *Listeria monocytogenes* and the protozoan *Toxoplasma gondii* [16].

In other studies, autophagy has been demonstrated to be critical in the destruction of a parasite-containing vesicular structure through the recruitment of immunity-related GTPases to the parasitophorous vacuole.

Several different immune signals positively regulate autophagy, including double-stranded RNA-activated protein kinase (PKR), Toll-Like Receptors (TLRs), tumor necrosis factor, the CD40–CD40L interaction, interferon-gamma (IFN-γ) and the immunity-related GTPases [16, 17,18, 19, 20] whereas T helper type 2 cytokines (IL-4 and 1L-13) negatively regulate autophagy [21].

Of particular interest is the connection between TLRs and the autophagy pathway [22]. Even if the physiological function of TLR-mediated

induction of autophagy is not yet known, it has been shown that TLRs can regulate autophagy [23, 24]. Moreover, the autophagic machinery can be used to deliver viral genetic material to endosomal TLRs for efficient induction of type I interferon40, and TLRs may act in the recruitment of autophagy proteins to phagosomal membranes [25].

Autophagy is also involved in the innate immune signaling, as demonstrated by the pivotal role of Atg5 in the production of type I interferon in plasmacytoid dendritic cells [26]. On the other hand, several studies have shown that absent expression of autophagy genes can result in enhanced production of type I interferon or other cytokines, including proinflammatory molecules such as IL-1β and IL-18, or adipocytokines, such as leptin and adiponectin [27, 28, 29, 30].

Moreover, macrophages from mice lacking Atg16l1 have increased production of proinflammatory cytokines IL-1β and IL-18 after endotoxin stimulation of TLR4 [27].

Recent findings demonstrate that autophagy is one of the mechanism for MHC class II presentation of certain endogenously synthesized peptides [17, 31]; moreover autophagy and the Atg5 protein seem to be involved in MHC class I–restricted antigen presentation [32].

Thymic selection is another important process that is proven to be associated with autophagy. It has been demonstrated that autophagy-dependent endogenous loading of MHC class II is important in shaping the

T cell repertoire. Thymic epithelial cells that function in positive and negative selection show constitutive autophagy, as demonstrated by the presence the green fluorescent protein–LC3 dots [33, 34].

During positive and negative selections, thymic epithelial cells present self-antigens to lymphocytes. Because thymic epithelial cells are not thought to have phagocytic activity, it is reasonable to hypothesize that they provide self-antigens from their own cytoplasm. In this scenario, autophagy in thymic epithelial cells might be involved in T-cell development and central tolerance [33].

Normal thymic T cell selection requires Atg5 expression in the stromal cells in thymic allografts [34]. Experiments with thymic transplantation show that the selection of MHC class II–dependent TCRs requires Atg5. Furthermore, mice with *Atg5*$^{-/-}$ thymic implants develop autoreactive CD4$^{+}$ T cells, as measured both by the proportion of CD62L$^{lo}$ peripheral cells and the development of inflammatory infiltrates in many organs, including the intestine. The development of autoreactive CD4$^{+}$ T cells in mice with *Atg5*$^{-/-}$ thymic implants is thought to reflect a function of Atg5 and, presumably, the autophagy pathway in controlling the repertoire of self peptides presented by thymic epithelial cells that are responsible for normal thymic selection and the generation of T cell tolerance. However, autophagy genes other than *Atg5* have not yet been analyzed in similar

studies, and thus the function of the cellular process of autophagy in thymic selection remains to be defined [35].

Autophagy plays a critical role in lymphocyte biology. Indeed, several studies have shown that deletion of autophagy genes in T lymphocytes and B lymphocytes alters their development, survival and/or function.

The thymus is a site of constitutive autophagy [33, 34], and the expression of Beclin 1 is regulated during T cell and B cell development and T cell activation [36]. For example, loss of Atg5 or Atg7 impairs the survival and proliferation of mature T lymphocytes in vivo [37-39], and Atg5 is required in B lymphocytes for the survival of developing pre–B cells in the bone marrow and of mature B-1a cells in the periphery [40]. One mechanism postulated for the involvement of Atg7 and Atg5 in the survival of mature T cells involves a classical autophagy function in the clearance of mitochondria and consequent prevention of the accumulation of reactive oxygen species and imbalance of the expression of pro- and antiapoptotic proteins [37, 39]. Notably, the developmental pattern of Beclin 1 in B lymphocytes, similar to that of the antiapoptotic protein Bcl-2, shows downregulation at the transition from pro–B cell to pre–B cell [41].

A controversial area is whether autophagy is exclusively a prosurvival pathway in lymphocytes or whether it also can be used as a death pathway. The impaired survival of certain populations of B cells or T cells [37, 38, 39, 40] following deletion of Atg5 or Atg7 suggests a major role for

autophagy in lymphocyte survival. However, it has been hypothesized that IFN-γ may induce Irgm1-regulated autophagic cell death in $CD4^+$ T cells [42]. In addition, knockdown of the gene encoding Beclin 1 or Atg7 results in less death of $CD4^+$ T cells induced by growth-factor withdrawal [43], and autophagy genes are required for the death of bystander $CD4^+$ T cells triggered by the human immunodeficiency virus envelope protein [44]. Thus, a consensus is growing that autophagy may mediate activation-induced death of $CD4^+$ T cells [35].

## 1.3 TRPV CHANNELS IN THE IMMUNE SYSTEM

The transient receptor potential proteins (TRPs) is a family of ion channels responsible for a wide array of cellular functions. Originally identified in Drosophila melanogaster, these channels are ubiquitously distributed throughout the mammalian system. Based on sequence similarity, the TRP superfamily can be divided into seven families (Fig.2): TRPC (canonical), TRPV (vanilloid), TRPM (melastatin), TRPN (Drosophila NOMPC) and TRPA (ankyrin), TRPML (mucolipin) and TRPP (polycystin).

**Fig.2** The TRP channels superfamily. Adapted from [45].

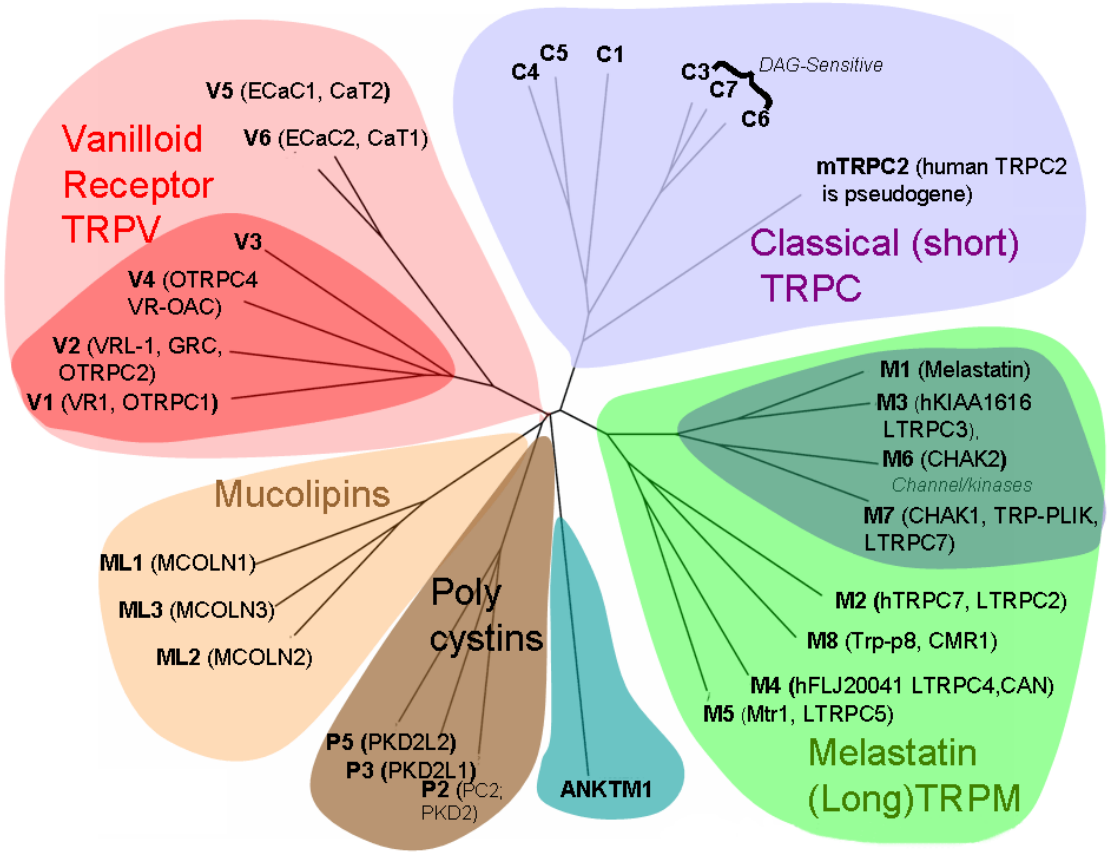

Each of these subfamilies contains several members which differ for mode of activation and response to stimuli. The general topology of a TRP subunit includes intracellular N- and C- terminal regions of variable length and six transmembrane spanning domains with a pore loop between transmembrane domain 5 and 6 [46]. Several families have a variable number of ankirin motifs within their intracellular N- termini, which are thought to participate in protein-protein interactions; members of individual TRP families may also share other motifs, such as coiled-coil domains [47]. The TRP subunits are thought to assemble as homo- or hetero-tetramers to form cation selective channels [48]: experimental evidence for tetramer formation exists for TRPV1, TRPV2 and TRPV5/6 [49, 50] and many TRPC channels can form heteromeric channels [51-53].

TRP channels are activated by a wide range of stimuli including intra- and extracellular messengers, chemical, mechanical and osmotic stress, temperature, growth factors and depletion of intracellular calcium stores [45]. The biophysical characterization of TRPs has revealed significantly different activation mechanisms and selectivity between channels. Functional studies have demonstrated that TRPs are necessary for a number of physiological processes, including sensation (such as taste, smell and temperature), hormone secretion and development. In table 1 are listed the main physiological function of TRP channels, reviewed in [54].

**Table 1.** TRP channel functions.

| TRP Subafmily | Physiological role |
|---|---|
| TRPC | • Regulation hepatocyte cell volume and endothelial permeability |
| | • Neural development |
| | • Regulation of vascular smooth cell proliferation |
| | • Proliferation of pulmonary artery endothelial cells |
| | • Activation of cystic fibrosis transmembrane conductance factor in vascular endothelial cells |
| | • Degranulation of mast cells |
| TRPV | • Nociception |
| | • Heat sensation |
| | • Inflammation |
| | • Ca2+ reabsorption in kidneys and bone |
| TRPM | • Insulin secretion |
| | • Allergic reactions |
| | • Migration of dendritic and mast cells |
| | • Inflammation |
| TRPA | • Mechanosensation |
| | • Cochlear amplification of sound |
| TRPML | • Vesicular transport |
| | • Control of pH in lysosomes |
| TRPP | • Mechanosensation |
| | • Follicle maturation and differentiation |

TRPV1 is predicted to have six transmembrane (TM) domains and a short, pore-forming hydrophobic stretch between the fifth and sixth TM domains [55]. Like many other TRP channels, TRPV1 has a long amino terminus containing three ankyrin-repeat domains and a carboxyl terminus containing a TRP domain close to the sixth TM. The ankyrin repeats consist of an 33-residue motif named after the cytoskeletal protein ankyrin, which contains 24 copies of these repeats. In other membrane proteins, ankyrin repeats are known to bind to many cytosolic proteins [56]. To date, one protein, calmodulin (CaM), has been reported to bind to the ankyrin

repeat domain of TRPV1 (the first ankyrin repeat) [57]. The Drosophila TRP channels form a heteromultimeric channel complex. These complexes, in turn, form part of a larger signaling complex that also contains a G protein-coupled receptor (rhodopsin), an effector (phospholipase C; PLC), regulators (protein kinase C; PKC and CaM), and the scaffolding protein INAD (inactivation no-after potential D) [58].

TRPV1 is also presumed to consist of a multimeric channel, though experimental evidence along these lines has been relatively limited. Oligomer formation analysis using perfluorooctanoic acid polyacrylamide gel revealed that TRPV1 forms multimers with a homotetramer as the predominant form (Fig. 3) [59]. Tetrameric stoichiometry for the native capsaicin receptor has also been suggested by the behaviour of a dominant negative TRPV1 mutant bearing amino acid substitutions in the sixth TM domain [60]. TRPV1 is also thought to form heterooligomers with TRPV3, another heat-sensitive TRP channel, based on the observations that TRPV3 is transcribed from a gene adjacent to TRPV1, is co-expressed in dorsal root ganglion (DRG) neurons with TRPV1, co-precipitates with TRPV1 in heterologous expression systems and may reduce TRPV1 responsiveness to capsaicin [61]. However, TRPV1 expressed alone in human embryonic kidney-derived HEK293 cells or Xenopus oocytes can account for the majority of the electrophysiological properties exhibited by native capsaicin receptors in sensory neurons, including ligand affinity,

permeability sequence, current/voltage (I/V) relationship, conductance and open probability at both single-channel and whole-cell levels. These results suggest either that TRPV1 can form homomultimers without other subunits [55, 62-65] or that incorporation of subunits other than TRPV1 does not influence the functional properties. I/V relationships in the whole-cell configuration have reversal potentials close to 0 mV, indicating the opening of non-selective cationic channels, and exhibit substantial outwards rectification with a region of negative slope conductance at potentials negative to 70 mV [62]. The open-time distributions of single-channel currents in the presence of low capsaicin concentrations (10–30 nM) are best fitted with three exponential components, while the closed-time distributions are best fitted by five exponential components, although number of exponential components seems to be different at higher capsaicin concentrations (0.5–1 μM) [64]. These single channel properties suggest the complex kinetics of TRPV1 channel gating. However, the single-channel properties show no significant differences between the native (sensory neurons) and cloned receptors, indicating again that functional native TRPV1 channels are made up of TRPV1 subunits.

Capsaicin (CPS), piperidine, eugenol, gingerol, resiniferatoxin, Δ9-tetrahydrocannabinol and cannabidiol as well as noxious heat (>43-45°C) have been found to act as exogenous TRPV1 agonists. In addition, endovanilloids, biogenic amines like N-arachidonylethanolamine, N-

arachidonoyldopamine and products of lipoxygenases (12-HETE and leukotriene B4) are described as endogenous vanilloid agonists [55, 66] (Fig.3).

**Fig. 3** Activation of TRPV1 by different endogenous or exogenous agonists [67].

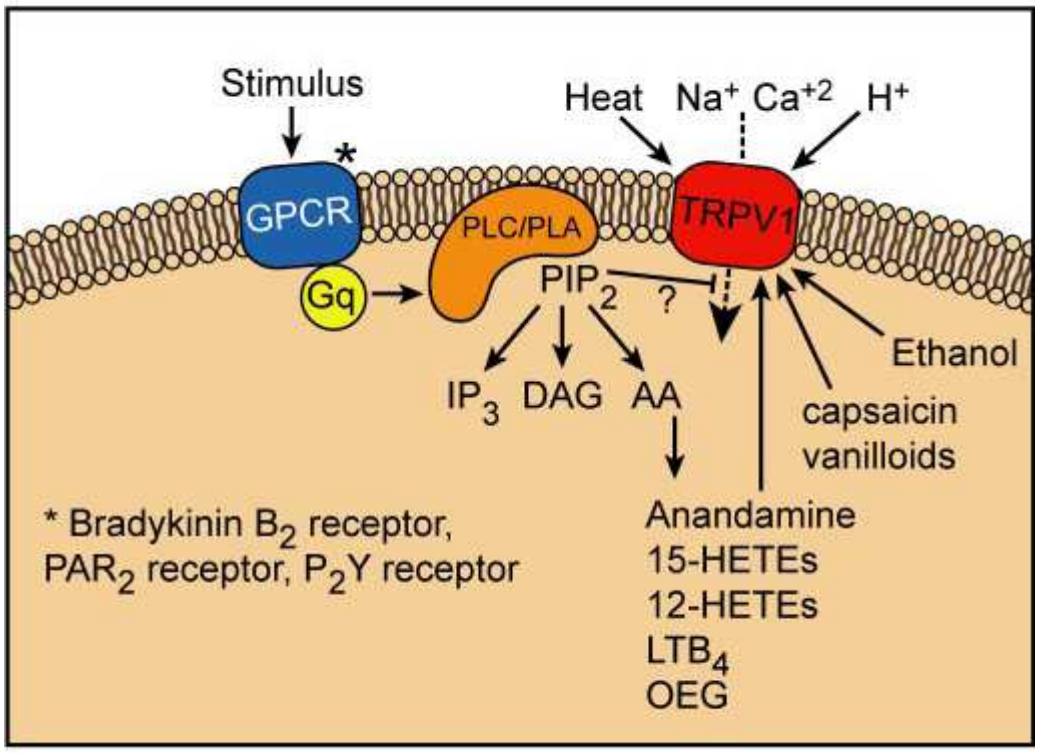

An increase in the intracellular calcium concentration ($[Ca^{2+}]_i$) is critical for lymphocyte activation that includes cell proliferation and differentiation [68] and [69]. In B and T lymphocytes, stimulation via an antigen receptor results in a biphasic Ca2+ response: an initial transient increase in $[Ca^{2+}]_i$ that corresponds to Ca2+ release from the endoplasmic reticulum (ER) store and the subsequent prolonged $[Ca^{2+}]_i$ elevation that depends on the $Ca^{2+}$ influx from the extracellular environment across the plasma membrane. Elevated $[Ca^{2+}]_i$ levels result in the activation of many transcription factors such as NF-AT and NF-κB, thereby leading to cell proliferation and production of various cytokines.

Several ion channels play an important role in increasing $[Ca^{2+}]_i$ in lymphocytes [70]. In the initial phase of $[Ca^{2+}]_i$ increase, the inositol 1,4,5-trisphosphate (IP3) receptor that is activated by IP3 is cleaved from phosphatidylinositol 4,5-bisphosphate (PIP2), thereby causing the release of $Ca^{2+}$ from the ER into the cytoplasm. In the subsequent phase, various ion channels cooperatively induce extracellular $Ca^{2+}$ influx across the plasma membrane and maintain increased $[Ca^{2+}]_i$. The store-operated channels (SOCs) including $Ca^{2+}$release-activated $Ca^{2+}$ channels (CRAC channels) are activated by the depletion of the $Ca^{2+}$ store; these channels are believed to contribute toward the maintenance of $[Ca^{2+}]_i$. Voltage-gated and $Ca^{2+}$-activated $K^+$ channels appear to contribute to the

hyperpolarization of the membrane potential that maintains the driving force of the $Ca^{2+}$ influx.

TRP channels have been reported to play important roles in $[Ca^{2+}]_i$ increase in lymphocytes [71], [72] and [73]. For example, in the avian B lymphocyte cell line DT40, the disruption of TRPC1 results in the reduction of both Ca2+ oscillations and the subsequent NF-AT activation caused by BCR ligation. TRPM4, a $Ca^{2+}$-activated monovalent-selective channel, contributes to $Ca^{2+}$ oscillation by regulating the membrane potential in Jurkat T cells. TRPC7 appears to function as a DAG-activated channel in DT40 B cells.

TRP channels have also been found to regulate thymopoiesis. Recently, it has been demonstrated that tissue-specific deletion of TRPM7 in T cell lineage disrupts thymopoiesis, with a developmental block of thymocytes at double-negative (DN) stage, and progressive depletion of thymic medullary cells [74]. In addition, some endogenous vanilloid agonists have been described in the thymus [75]. Moreover, we have previously reported that treatment with CPS affects T cell differentiation and functions in a TRPV1-dependent manner, by regulating the apoptosis of distinct thymocyte subpopulations [76].

# 2. AIM OF THE WORK

Given this background, aim of the study was to investigate the role of TRPV1, a member of the family of cation channels of increasing interest, in the regulation of the autophagic/apoptotic processes and its potential involvement in thymocyte development.

# 3. MATERIALS AND METHODS

## 3.1 ANIMALS

C57Bl/6 male mice were purchased from Harlan, Udine, Italy. GFP-LC3 [33] and Beclin-$1^{+/-}$ mice [77] were provided by Prof. Francesco Cecconi (Tor Vergata University, Rome, Italy) and housed as previously described [76]. Five animals, 6-10 weeks-old, were sacrificed for each experiment in accordance with the National Institutes of Health 'Guidelines for the Care and Use of Laboratory Animals'.

## 3.2 CELL PREPARATION

Thymi were teased and cellular debris was removed by extensive washing. Thymocytes were isolated by centrifugation on Lympholite-M (Cederlane, Burlington, Canada) gradient, washed twice in RPMI-1640 medium (Lonza, Basel, Switzerland) containing 10% heat-inactivated fetal bovine serum (FBS), 2 mM L-glutamine, 100 IU/ml penicillin, 100 mg streptomycin (Lonza), counted and diluted at appropriate concentrations in medium. Cell purity (99%) was assessed by immunofluorescence and FACS analysis using anti-CD3 monoclonal antibody (mAb).

## 3.3 REAGENTS

The following monoclonal antibodies (mAbs) were used: PE-conjugated anti-mouse CD3, PE-conjugated anti-mouse CD4 (CD4-PE), CyChrome-conjugated anti-mouse CD8 (CD8-CyChrome) (1 µL/1x$10^6$ cells), anti-caspase-3 (1:1000, BD Biosciences, San Josè, CA, USA), anti-Bcl-$X_L$ (1:200) and anti-actin (1:1000) (Santa Cruz Biotechnology, Santa Cruz, CA), and rabbit anti-phospho AMP-activated kinase (AMPK) (1:1000, p-AMPK) (Cell Signaling Technology, Danvers, MA, USA). The following rabbit polyclonal Abs were used: anti-TRPV1 (western blot 1:200; flow cytometry 1:25; Abcam, Cambridge, MA), anti-AMPK, anti-ATG4C and anti-Beclin-1 (1:1000, Cell Signaling), anti-LC3 (2 µg/mL, Novus Biologicals, Littleton, CO). Fluorescein isothiocyanate (FITC)-conjugated goat anti-rabbit (GARB, 1:20) from Santa Cruz Biotechnology. Horseradish peroxidase (HRP)-conjugated sheep anti-mouse (1:2000) and HRP-conjugated donkey anti-rabbit (1:20000) from GE Healthcare Bio-Sciences AB (Uppsala, Sweden). z-VAD (OMe)-FMK from Enzo Life Sciences (Farmingdale, NY). FLUO 3-AM (7 µM) and acridine orange (AO, 1 □g/mL) were Invitrogen (San Diego, CA, USA). CPS (10 µM), capsazepine (CPZ, 1 µM), rapamycin (10 ng/ml), 3-methyl adenine (3-MA, 5 mM), bafilomycin A1 (1 µM), compound C (10 µM), ethylenediaminetetraacetic acid (EDTA, 5 mM), N-acetylcysteine (NAC,

10 mM), 2',7'-dichlorofluorescein diacetate (DCFDA, 10 μg/ml), Trypan blue and dimethyl sulfoxide (DMSO) from Sigma-Aldrich.

### 3.4 FLOW CYTOMETRY

To determine the expression of TRPV1 on mouse thymocytes, 5x105 cells were fixed and permeabilized using CytoFix/CytoPerm Plus (BD Biosciences) before the addition of anti-TRPV1 polyclonal Ab. Normal goat serum was used as negative control. After 20 min at 4 °C, cells were washed twice and labelled with FITC-conjugated GARB.

In some experiments, thymocytes from wild-type (wt) and GFP-LC3 transgenic mice [78] untreated, treated with CPS (10 μM) or pre-treated with 3-MA (5 mM) before the addition of CPS, were double stained with anti-CD4-PE and anti-CD8-CyCrome mAbs and analyzed on a FACScan cytofluorimeter (BD Biosciences). Electronic compensation was used between green, red and orange fluorescences to remove spectral overlaps. The percentage of positive cells was determined over 10,000 events and fluorescence intensity was expressed in arbitrary units on a logarithmic scale.

### 3.5 ACIDIC VESICULAR ORGANELLES (AVOs) DETECTION

AO is a cell-permeable lysosomotropic agent that fluoresces when excited with blue light. In its uncharged state AO emits green in the cytoplasm and

nucleus, and in its protonated form it accumulates inside acidic vesicles and emits red light. Briefly, 3x105 thymocytes were seeded into 24-well plates and cultured for the indicated times with CPS (10 μM) alone or in combination with CPZ (1 μM). In some experiments, thymocytes were pre-treated with 3-MA (5 mM) before the addition of CPS. At the end of treatments cells were washed with fresh medium, stained with AO and analyzed by flow cytometry as previously described [79].

### 3.6 CALCIUM INFLUX ($[Ca^{2+}]_i$) MEASUREMENT

Intracellular $Ca^{2+}$ flux was measured using FLUO 3-AM as previously described [76]. After FLUO 3-AM staining, cells were resuspended in RPMI/FCS medium supplemented or not with EDTA (5 mM), warmed to 37 °C for 5 min, and stimulated with 10 μM of CPS for different times. In some experiments, cells were treated with CPS in combination with CPZ (1 μM). FLUO-3 fluorescence was measured on the Flow cytometer at 525 nm on the green channel; untreated cells were analyzed to establish baseline fluorescence levels.

### 3.7 REACTIVE OXYGEN SPECIES (ROS) PRODUCTION

Thymocytes, untreated or treated with CPS (10 μM) for different times (5, 15, 30, 60 and 120 min), were cultured at a density of 1.5x105 in 24-well plates, washed with PBS, pulsed with DCFDA (10 μg/ml) for 10 min at 37

°C 5% CO2 and quickly analysed by Flow cytometry and the CellQuest Software. In some experiments, treated cells were cultured in the presence of NAC (10 mM), CPZ (1 μM) or EDTA (5 mM).

### 3.8 WESTERN BLOT

Lysates were obtained by using lysis buffer (1M Tris pH 7.4, 1M NaCl, 10 mM EGTA, 100 mM NaF, 100 mM Na3VO4, 100 mM PMSF, 2% deoxycholate, 100 mM EDTA, 10% Triton X-100, 10% glycerol, 10% SDS, 0.1M Na4P2O7) containing protease inhibitor cocktail (Sigma Aldrich) and the Mixer Mill MM300 (Qiagen, Hilden, Germany). Samples were separated on 7% SDS-PAGE, transferred onto Hybond-C extra membranes (GE Healthcare), blocked with 5% low-fat dry milk and blotted with rabbit anti-TRPV1 Ab followed by HRP-conjugated donkey anti rabbit Ab. In addition, proteins were separated on 14% SDS-PAGE and immunoblotted with rabbit anti-LC-3 or mouse anti-caspase-3 followed by the appropriate HRP-conjugated Abs. For the detection of AMPK, p-AMPK, Atg4C, Beclin-1 and Bcl-XL, lysates were separated on 10% SDS-PAGE. The detection was performed using the LiteAblot ®PLUS or the LiteAblot ®TURBO (EuroClone, Milano, Italy) kit and densitometric analysis by a Chemidoc using the Quantity One software (BioRad). Each sample was compared to its loading control (actin) for quantification.

## 3.9 IMMUNOPRECIPITATION AND OXYBLOT

Cell lysates (200 μg), from thymocytes untreated or treated for 2 h with CPS (10 μM) alone or in combination with NAC (10 mM), were precleared with protein A-sepharose (GE Healthcare) and then incubated overnight at 4°C with rabbit anti-Atg4C Ab (1:100) (Cell Signaling Technology) cross-linked to protein A. After washings, immunoprecipitated complex was eluted from beads and aliquots of immunoprecipitated Atg4C were derivatized using the Oxyblot Protein Oxidation Detection Kit (Millipore Corporation, Billerica, MA, USA). After neutralization, samples were applied on 10% SDS-PAGE, transferred and processed following the manufacturer's instructions. The detection and the densitometric analysis were performed as above described.

## 3.10 CELL VIABILITY

Thymocytes (1.5x106/ml) were seeded into 6-well plates and cultured for the indicated times with CPS (10 μM) or pre-treated with 3-MA (5 mM) before the addition of CPS at 37°C, 5% CO2. After treatment, cells were collected and labelled with 0.4% Trypan Blue solution (Sigma Aldrich). Enumeration of viable cells was carried out in Neubauer's chambers using a light microscope at 10X magnification.

## 3.11 DNA FRAGMENTATION

Time-course experiments of nucleosomal DNA fragmentation were performed by agarose gel electrophoresis. Briefly, 1.5x106/ml thymocytes were cultured at 37°C, 5% CO2 with or without CPS (10 μM) for the indicated times; thymocytes were also pre-treated with 3-MA (5 mM) before the addition of CPS. After treatment, cells were washed in PBS, and DNA was extracted using the Qiagen DNA extraction kit. The DNA samples were electrophoresed on ethidium bromide-stained 1.7% agarose gels and acquired by ChemiDoc.

Nucleosomal DNA fragmentation was also evaluated by the MEBSTAIN Apoptosis Kit Direct (MBL Medical and Biological laboratories CO., Naka-ku Nagoya, Japan) according to the manufacturer's instructions for Flow cytometry analysis, in thymocytes treated as above described and stained with anti-CD4-PE and anti-CD8-CyCrome mAbs. In brief, cells were fixed with 1% paraformaldehyde for 15 min on ice, washed, permeabilized with 70% ethanol for 15 min on ice, washed and then stained with the reaction mix for 30 min at 37°C.

## 3.12 RNA ISOLATION, REVERSE TRANSCRIPTION AND qRT-PCR ANALYSIS

Total RNA was extracted from untreated, CPS-treated thymocytes and from spleen tissue, by the RNeasy Mini Kit (Qiagen). RNA samples were

resuspended in RNAse-free water and their concentration and purity were evaluated by A260-A280 measurement. RNA samples (500 ng) were subjected to reverse transcription using the High Capacity cDNA Archive Kit (Applied Biosystems, Foster City, CA, USA) according to the manufacturer's instructions. One µl of the resulting cDNA products was used as template for RT-PCR quantification. Quantitative RT-PCR was performed using the iQ5 Multicolor Real-Time PCR Detection System (Biorad). The reaction mixture contained the SYBR Green PCR Master Mix (Biorad) and forward and reverse primers designed from sequences in the GeneBank database by Beacon Designer 5.1 software (Premier Biosoft International, Palo Alto, CA, USA): TRPV1: FW 5'-CTCCAGACAGA GACCCTAAC-3' RV 5'-TCTTCTGAGTCACCCTTCC-3'; Atg4A: FW 5'-TGGGTGGCCTTTGTTGTAACT-3', RV 5'-TGCTCGGTCACA TGCATATTG-3'; Atg4B: FW 5'-GGCCAGGAGCTATTGTGCTG-3', RV 5'-CCCCTTACTACCAACAACAGGAGT-3'; Atg4C: FW 5'-TGAA GTCCAGTAGTTACAGTTACG-3', RV 5'-AGCACAGCACACCGA AGC-3'; Atg4D: FW 5'-ACACAGGGTGCACTGGAGATG-3', RV 5'-TCAGCGAACCAGGAAACAATC-3'; glyceraldehyde-3-phosphate dehydrogenase (GAPDH): FW 5'-CCCACTAACATCAAATGGGG-3', RV 5'-TTGGCTCCACCCTTCAAGT-3'. Each PCR amplification consisted of 3 min at 94°C, followed by 40 cycles at 94°C for 15s, 58°C for 30s and 72°C for 30s. All controls and samples were assayed in triplicate in

the same plate. Measurement of GAPDH mRNA was used as control to normalize mRNA content.

### 3.14 RT-PCR PROFILER ARRAY

Total RNA from thymocytes, untreated or treated with CPS (10 μM) alone or with 3-MA, was isolated as above described. One microgram of the obtained RNA was subjected to RT using the Reaction Ready first strand cDNA kit (Superarray Bioscience Corporation, Frederick, MD) following the manufacturer's instructions. Quantitative RT-PCR was performed using the IQ5 Multicolor Real-time PCR detection system (Biorad), the RT2 real-time SYBR green PCR Mix and the Mouse Autophagy plates (Superarray Bioscience Corporation). Each PCR amplification consisted of heat activation for 10 min at 95 °C followed by cycles of 95 °C for 15 sec and 60 °C for 1 min. Measurement of five housekeeping genes on the samples was used to normalize mRNA contents and results were expressed as relative fold of the corresponding control.

### 3.15 STATISTICAL ANALYSIS

The statistical significance was determined by Student's t-test and by Anova with Bonferroni post-test. No statistical significative difference was found between untreated and vehicle (DMSO)-treated thymocytes (data not shown).

# 4. RESULTS

## CPS INDUCES AUTOPHAGY IN THYMOCYTES

Autophagy in the thymus is activated under stress conditions [80, 81]. CPS has been found to induce cellular stress [82], but at present no data on the ability of CPS to trigger an autophagic program in the thymus have been provided. Thus, we first determined whether treatment of thymocytes with CPS could induce autophagy as indicated by the processing of LC3. Ficoll-purified $CD3^+$ thymocytes (>99%) (data not shown), treated or not with CPS for different times, were analyzed for LC3 mobility. CPS caused a significative accumulation of lipidated LC3 (LC3-II) at 2h after treatment that declined thereafter (Fig. 4A). Similar results were obtained treating thymocytes with rapamycin used as positive control (data not shown).

Autophagy requires the formation of autophagosomes, which then fuse with endosomes/lysosomes to form AVOs, where degradation of the cargo occurs. Thus we detected AVOs formation by AO staining and flow cytometry. Time-course analysis on thymocytes exposed to CPS evidenced a significant level of AVOs formation at 2h as compared to untreated cells (Fig. 4B).

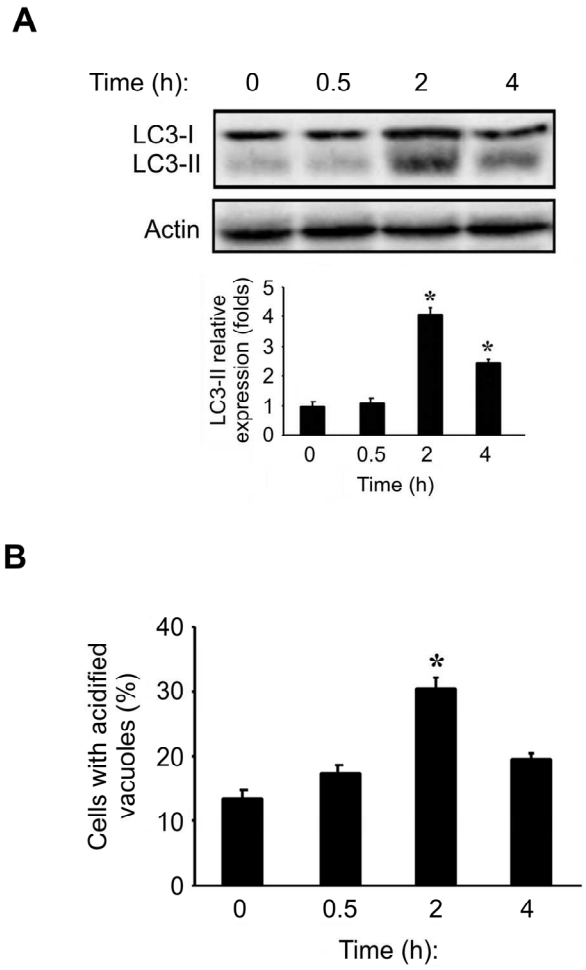


***Fig.4 CPS induces autophagy in mouse thymocytes.***
**A)** Lysates from thymocytes, untreated or treated with CPS for different times, were separated on 14% SDS-PAGE and probed with anti-LC3 Ab. One representative out of three independent experiments is shown. Statistics of densitometric analysis was performed by Anova Bonferroni post-test, *p<0,01.
**B)** The percentage of cells positive for AVOs was evaluated by AO staining and FACS in untreated or CPS-treated thymocytes. Data shown are the mean ± SD of three independent experiments; Anova Bonferroni post-test, *p<0,01.

## 4.2 CPS-INDUCED AUTOPHAGY IS TRPV1-DEPENDENT.

In order to analyze the involvement of TRPV1 in CPS-induced autophagy in thymocytes, we firstly evaluated the expression of TRPV1 mRNA qRT-PCR analysis. We found that thymocytes and spleen tissue, used as positive control [83], express the TRPV1 mRNA (Fig. 5A). The expression of TRPV1 was also assessed at protein level by Western blot and cytofluorimetric analyses. A band of apparent MW of 95 kDa (Fig. 5B), corresponding to TRPV1, was found in the lysates from thymocytes and positive control; no reactivity was observed with normal goat serum (data not shown). Furthermore, by FACS analysis we found that the majority of thymocytes express TRPV1 (Fig. 5C).

Finally, we analyzed the LC3 conjugation and AVOs formation in thymocytes treated for 2h with CPS alone or in combination with the specific TRPV1 inhibitor CPZ. We found that CPZ markedly reverted the CPS-induced autophagy (Fig. 5D, E), indicating this process is a TRPV1-mediated event.

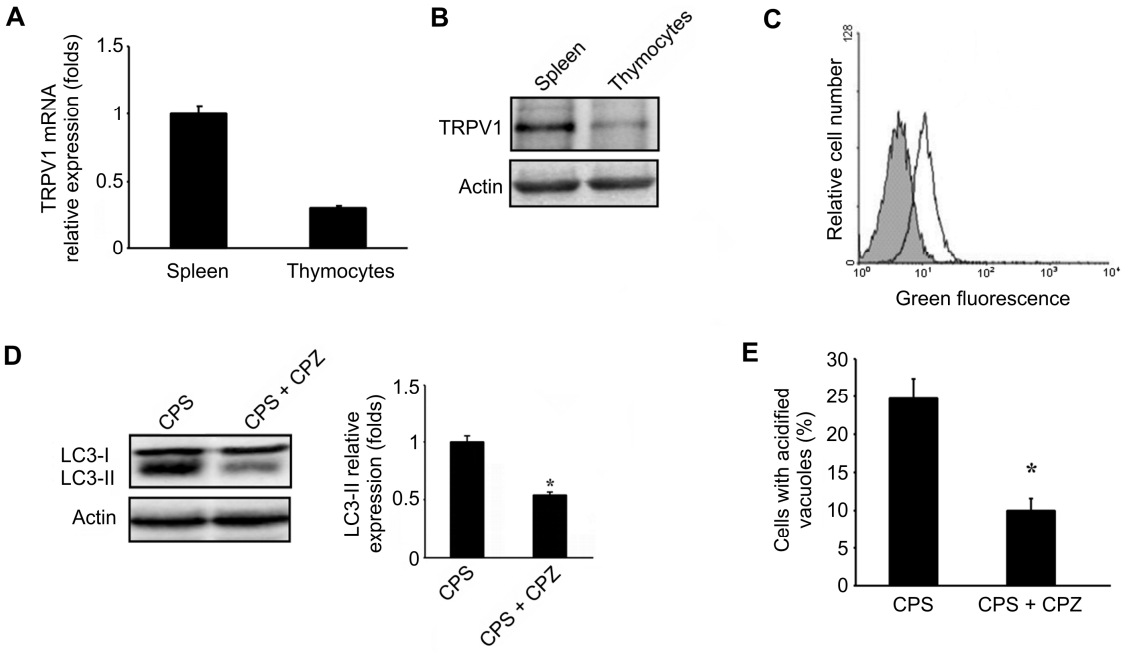


***Fig. 5 CPS induces autophagy in a TRPV1 dependent manner.***
**A)** TRPV1 mRNA levels on thymocytes and spleen tissue, used as control, were evaluated by qRT-PCR. TRPV1 levels are expressed as relative fold with respect to control. Data shown are the mean ± SD of three independent experiments.
**B)** Lysates from thymocytes and spleen tissue were separated on 7% SDS-PAGE and probed with anti-TRPV1 Ab. One representative out of three independent experiments is shown.
**C)** The expression of TRPV1 on thymocytes was evaluated by immunofluorescence and FACS analysis using anti-TRPV1 Ab. FITC-conjugated GARB was used as secondary antibody. Grey area shows secondary antibody alone. One representative out of three independent experiments is shown.
**D)** Lysates from thymocytes, treated for 2 h with CPS alone or in combination with CPZ were separated on 14% SDS-PAGE and probed with anti-LC3 Ab. One representative out of three independent experiments is shown. Statistics of densitometric analysis was performed by comparing CPS plus CPZ- with CPS-treated cells; Student's t-test, *p<0,01.
**E)** The percentage of cells positive for AVOs was evaluated by AO staining in thymocytes treated as described in panel D. Statistical analysis was assessed by comparing CPS plus CPZ- with CPS-treated cells; Student's t-test, *p<0,01.

## 4.3 TRPV1 ACTIVATION STIMULATES AUTOPHAGY IN A ROS- AND CALCIUM INFLUX ($[Ca^{2+}]_i$)-DEPENDENT MANNER.

Stimulation of TRPV1 of different cell types by CPS results in $[Ca^{2+}]_i$ mobilization and ROS production [82]. Thus, to characterize calcium transport through TRPV1, we followed CPS-induced $[Ca^{2+}]_i$ by cytofluorimetric analysis in thymocytes loaded with FLUO3. CPS stimulation of thymocytes in $Ca^{2+}$-containing medium induced a rise of $[Ca^{2+}]_i$ from 170 to 500 nM. The kinetics of mobilization showed that CPS induces a rapid response (3 min) that peaks at 6 min and declines thereafter. We also examined the source of calcium responsible for these changes by stimulating thymocytes with CPS in the presence of the extracellular chelator EDTA (nominally Ca2+-free medium). Under these conditions, the ability of CPS to induce $Ca^{2+}$ mobilization was completely blocked. Similar results were obtained by using CPS in combination with CPZ, indicating that Ca2+ response was mediated by TRPV1 (Fig. 6A). Then, we measured the CPS-induced ROS production in thymocytes using DCFDA and FACS analysis. CPS induced a sustained ROS accumulation that begins at 15 min and increases at later time points (Fig. 6B); moreover, the ROS scavenger NAC completely inhibited ROS production, indicating that thymocytes accumulate peroxides under these conditions (Fig. 6C).

Given that thymocytes generate ROS in response to $[Ca^{2+}]_i$ increase [84], we then analysed whether the TRPV1-dependent $[Ca^{2+}]_i$ rise could be

essential for CPS-induced ROS by evaluating the effect of CPZ or EDTA. As expected, CPZ and EDTA completely inhibited ROS production in CPS-treated cells (Fig. 6C).

Finally, we explored whether the [Ca2+]i rise and ROS were essential for autophagy in thymocytes, by assaying the effect of EDTA or NAC on the formation of autophagosomes using LC3 as marker. Addition of EDTA or NAC to thymocytes for 30 min before CPS-treatment resulted in a marked reduction of LC3 lipidation (Fig. 6D).

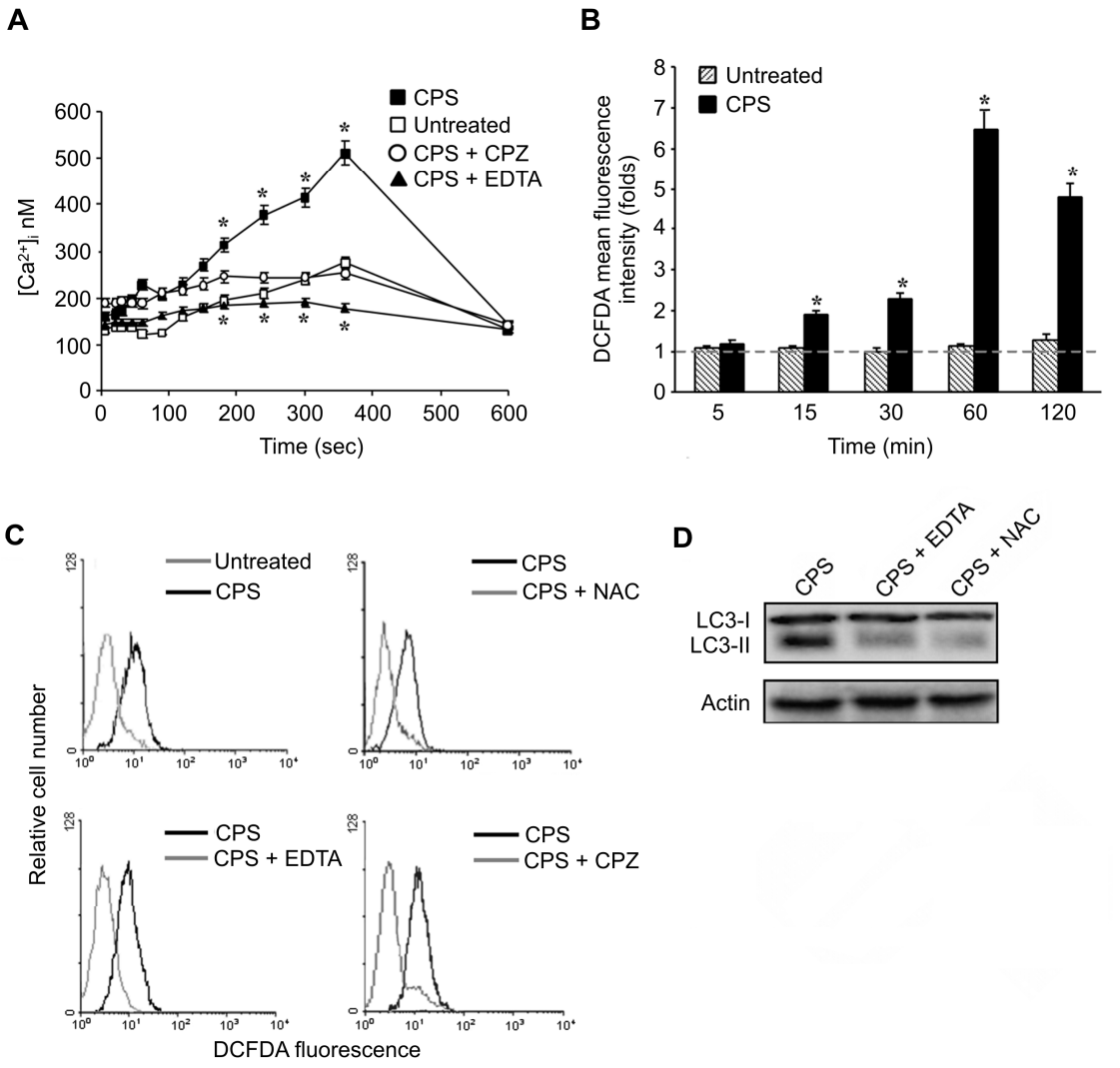


***Fig. 6 TRPV1 triggering by CPS induces $[Ca^{2+}]_i$ and ROS production leading to autophagy.***

**A)** Time course of $[Ca^{2+}]_i$ rise in FLUO 3-loaded thymocytes, untreated or treated with CPS alone or in combination with CPZ or with EDTA was evaluated by FACS analysis. Data shown are the mean ± SD of three independent experiments. Statistical analysis was determined by comparing CPS-treated with untreated thymocytes and CPS plus CPZ- or CPS plus EDTA- with CPS-treated cells; Anova Bonferroni post-test, *p<0,01.

**B)** ROS production was evaluated in thymocytes, untreated or treated with CPS for different times, by DCFDA staining and FACS analysis. Data, shown as the mean ± SD of three independent experiments, are expressed as fold change with respect to ROS basal level (time 0, dot line) used as control. Statistical analysis was determined by comparing untreated with control and CPS-treated with untreated cells; Anova Bonferroni post-test, *p<0,01.

**C)** ROS production was assayed as above described in thymocytes treated for 1 h with CPS, alone or in combination with NAC, EDTA or with CPZ. One representative out of three independent experiments is shown.

**D)** Lysates from thymocytes, treated for 2 h with CPS alone or in combination with EDTA or NAC were separated on 14% SDS-PAGE and probed with anti-LC3 Ab. One representative out of three independent experiments is shown.

## 4.4 TRPV1 TRIGGERING BY CPS REQUIRES AMPK ACTIVATION FOR AUTOPHAGY INDUCTION.

The energy sensor AMPK acts as a major regulator of cellular adenosine-5'-triphosphate levels and protects cells against stresses. Recent evidence demonstrates that activation of AMPK by $Ca^{2+}$ and ROS signaling inhibits the mammalian target of rapamycin (mTOR) complex and induces autophagy [85]. Given that phosphorylation of Thr-172 of AMPK is necessary for its activity [86], the phosphorylation status of AMPK in untreated and CPS-treated thymocytes was measured. Time-course immunoblot analysis showed that enhancement of AMPK phosphorylation occurs rapidly being evident at 5 min and peaking at 15 min after CPS exposure (Fig. 7A). Moreover, we treated thymocytes with CPS in the presence of EDTA or NAC and found that both compounds markedly reverted the CPS-induced AMPK phosphorylation (Fig. 7B). Finally, we evaluated the involvement of AMPK activation in CPS-induced autophagy by using the AMPK inhibitor compound C that completely blocked the LC3 lipidation (Fig. 7C).

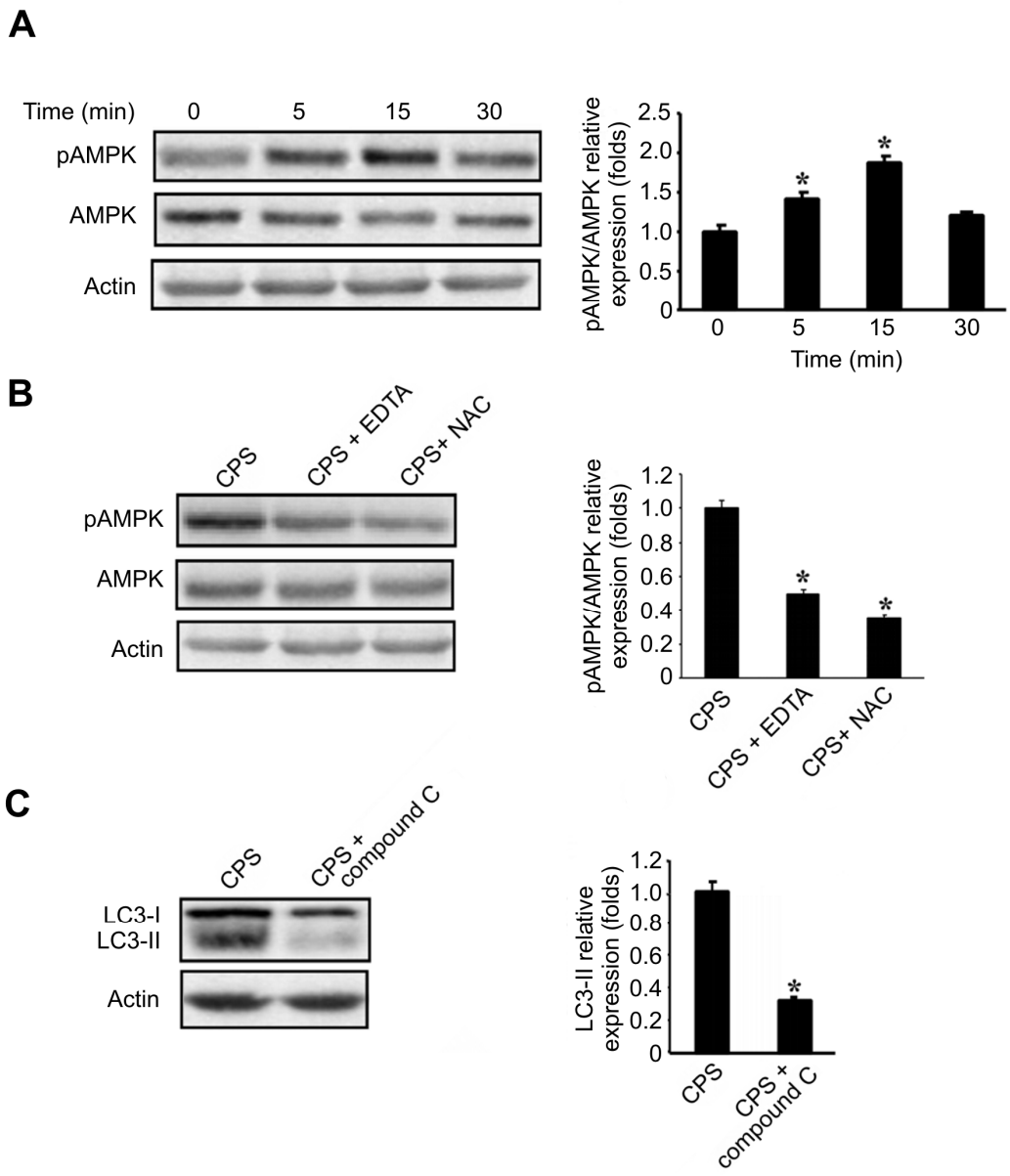


***Fig. 7 CPS induced-autophagy in thymocytes requires AMPK activation.***
**A)** Lysates from thymocytes treated for different times with CPS, were separated on 10% SDS-PAGE and probed with anti-pAMPK mAb and anti-AMPK Ab. Statistics of densitometric analysis was determined by Anova Bonferroni post-test, *p<0,01.
**B)** Lysates from thymocytes treated for 15 min with CPS, alone or in combination with EDTA or NAC were analyzed as above described. Statistics of densitometric analysis was assessed by comparing CPS plus EDTA- or CPS plus NAC- with CPS-treated cells. Student's t-test, *p<0,01.
**C)** Lysates from thymocytes, treated for 2 h with CPS alone or in combination with compound C were separated on 14% SDS-PAGE and probed with a rabbit anti-LC3 Ab. Statistical analysis was determined by comparing CPS plus compound C- with CPS-treated cells. Student's t-test, *p<0,01.
One representative out of three independent experiments is shown in each panel.

## 4.5 CPS TREATMENT OF THYMOCYTES AFFECTS AUTOPHAGIC GENE EXPRESSION.

To evaluate the effects of CPS on autophagic gene expression in thymocytes, we performed a RT-Profiler array in cells untreated, treated for 2h with CPS or pre-treated for 30 min with 3-MA before the addition of CPS. At 2h after CPS treatment, Atg4C gene was up-regulated. In addition, CPS plus 3-MA induced a strong Atg4C, Irgm1 and Bcl2L1 genes down-regulation (Table 2).

**Table 2.** CPS treatment affects autophagic gene expression.

| Description | CPS vs DMSO (Fold change) | CPS plus 3-MA vs CPS (Fold change) |
|---|---|---|
| Autophagy related 4C (yeast) | 5.00 ± 1.04 | -4.62 ± 1.38 |
| Bcl2-like 1 | - | -2.63 ± 0.45 |
| Immunity-related GTPase family M member 1 | - | -2.59 ± 0.34 |

- : no changes.

## 4.6 CPS INDUCES ATG4C OXIDATION IN THYMOCYTES IN A ROS-DEPENDENT MANNER.

The cysteine protease family of Atg4s represents the main cellular target of oxidative signals in autophagy, and their delipidating activity is tightly regulated by changes in ROS concentrations, specifically $H_2O_2$ which is essential for autophagosome formation [87]. RT-Profiler assay results were confirmed by qRT-PCR. We found that thymocytes express the four mammal Atg4 paralogues (A, B, C and D) and that CPS treatment specifically increased the Atg4C mRNA expression alone (Fig. 8A). Given that Atg4 activity is regulated by oxidation, we immunoprecipited the Atg4C protein from lysates of thymocytes untreated or treated for 2h with CPS alone or in combination with NAC and analyzed its oxidation status.

We found that TRPV1 activation by CPS triggers oxidation of Atg4C with a concomitant regulation of LC3 lipidation levels (Fig. 8B) in a ROS-dependent manner, suggesting that ROS-mediated induction of autophagy involves Atg4C activity.

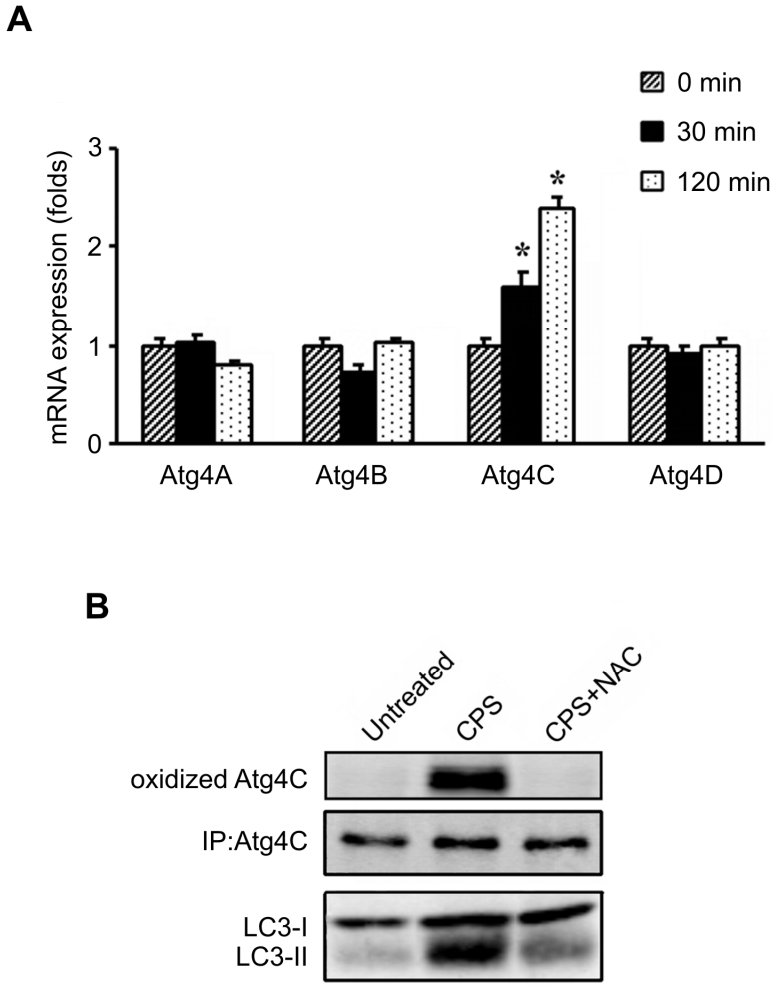


***Fig. 8 ROS signaling induces oxidation of Atg4C in CPS-treated thymocytes.***
**A)** Atg4 A, B, C and D mRNA levels were evaluated in thymocytes, untreated or treated for different times with CPS by qRT-PCR. Levels of each Atg4 are expressed as relative fold with respect to untreated cells used as control. Data shown are the mean ± SD of three independent experiments. Statistical analysis was performed by Anova Bonferroni post-test, *p<0,01.
**B)** Oxidation levels were evaluated in lysates, from thymocytes untreated or treated for 2h with CPS alone or in combination with NAC, immunoprecipitated with anti-Atg4C Ab. Aliquots of immunoprecipitated Atg4C were derivatized, separated on 10% SDS/PAGE and processed according to the kit instructions. Lysates were also separated on 14% SDS-PAGE and probed with anti-LC3 Ab. One representative out of three independent experiments is shown.

## 4.7 INVOLVEMENT OF BECLIN-1 IN AMPK-DEPENDENT CPS-INDUCED AUTOPHAGY

Beclin-1 plays an essential role in maintaining normal thymic cellularity [88]. Thus, we evaluated the involvement of Beclin-1 in TRPV1-mediated autophagy using Beclin-$1^{+/-}$ transgenic mice, founding that CPS-treated thymocytes show lower LC3-II levels as compared to their wild-type counterparts (Fig. 9A).

Since Beclin-1 up-regulation occurs during the autophagic process [89], we performed a time-course analysis of Beclin-1 expression in CPS-treated thymocytes and found that Beclin-1 protein expression increases after 1-2h of treatment (Fig. 9B). In addition, the treatment with CPZ, NAC or compound C markedly reverted CPS-induced effects, indicating that Beclin-1 upregulation is dependent by TRPV1 triggering, ROS generation and AMPK activation (Fig. 9C).

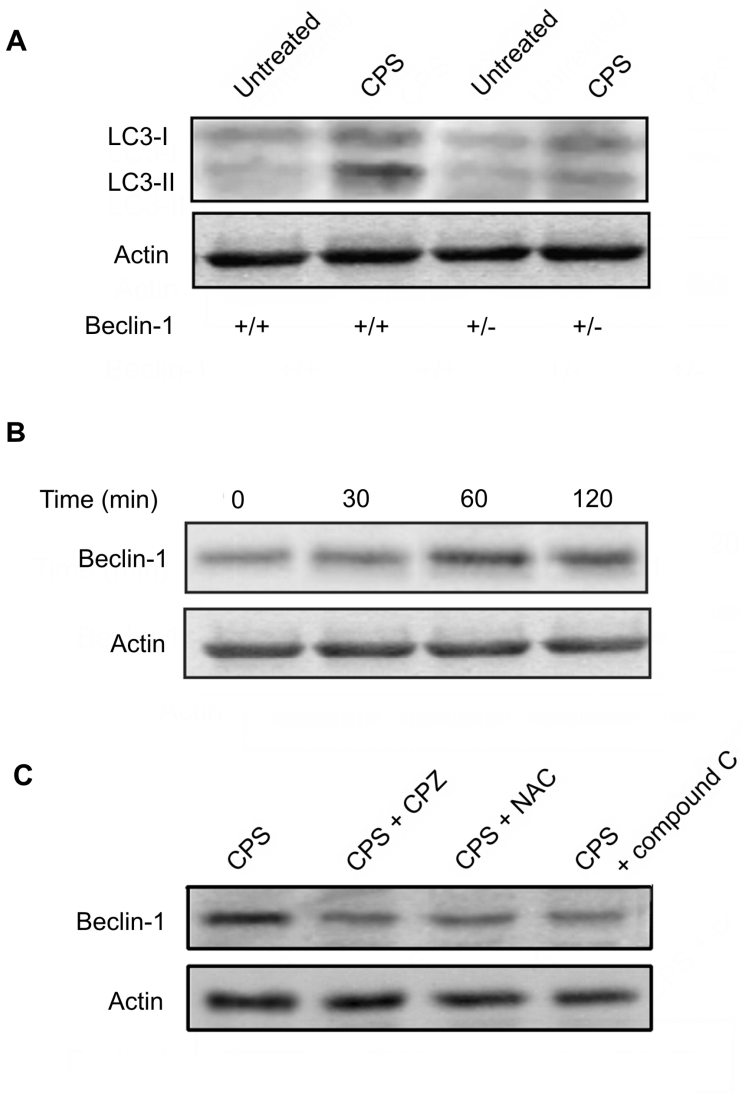


***Fig. 9 Involvement and regulation of Beclin-1 in CPS-induced autophagy***

**A)** Lysates from wild type and Beclin-$1^{+/-}$ thymocytes, untreated or treated with CPS for 2 h, were separated on 14% SDS-PAGE and probed with anti-LC3 Ab.

**B)** Lysates from thymocytes, treated for different times with CPS were separated on 10% SDS-PAGE and probed with anti-Beclin-1 Ab.

**C)** Lysates from thymocytes, untreated or treated for 2 h with CPS alone or in combination with CPZ, NAC or compound C, were separated on 10% SDS-PAGE and probed with anti-Beclin-1 Ab.

## AUTOPHAGY IS REQUIRED FOR THYMOCYTE SURVIVAL UPON TRPV1 ACTIVATION

Autophagy can either mediate cell death or act as pro-survival mechanism depending on cellular contexts and stimuli [90]. Thus, we evaluated the result of CPS-induced autophagy in term of survival or death of thymocytes. As demonstrated by Trypan Blue exclusion assay, CPS treatment did not affect thymocyte viability (Fig. 10A). Furthermore, pretreatment of thymocytes with the autophagic inhibitor 3-MA, or with bafilomycin A1 (data not shown), reverted the CPS-induced autophagy, as evaluated by reduction of LC3-II levels (Fig. 10B, C), decreased the total thymocyte number (Fig. 10D), and induced DNA fragmentation (Fig. 10E). No cytotoxicity was detected with 3-MA alone. Moreover, pre-incubation with 3-MA resulted in down-regulation of Beclin-1 and Bcl-XL protein levels and caspase-3 activation (Fig 10F, G). Finally, pretreatment with z-VAD, a pancaspase inhibitor, completely reverted the 3-MA-induced Beclin-1 down-regulation in CPS-treated thymocytes, suggesting that Beclin-1 degradation and induction of apoptosis are caspase-dependent events (Fig. 10G). Overall these findings demonstrate that CPS-induced autophagy acts as a pro-survival mechanism in thymocytes.

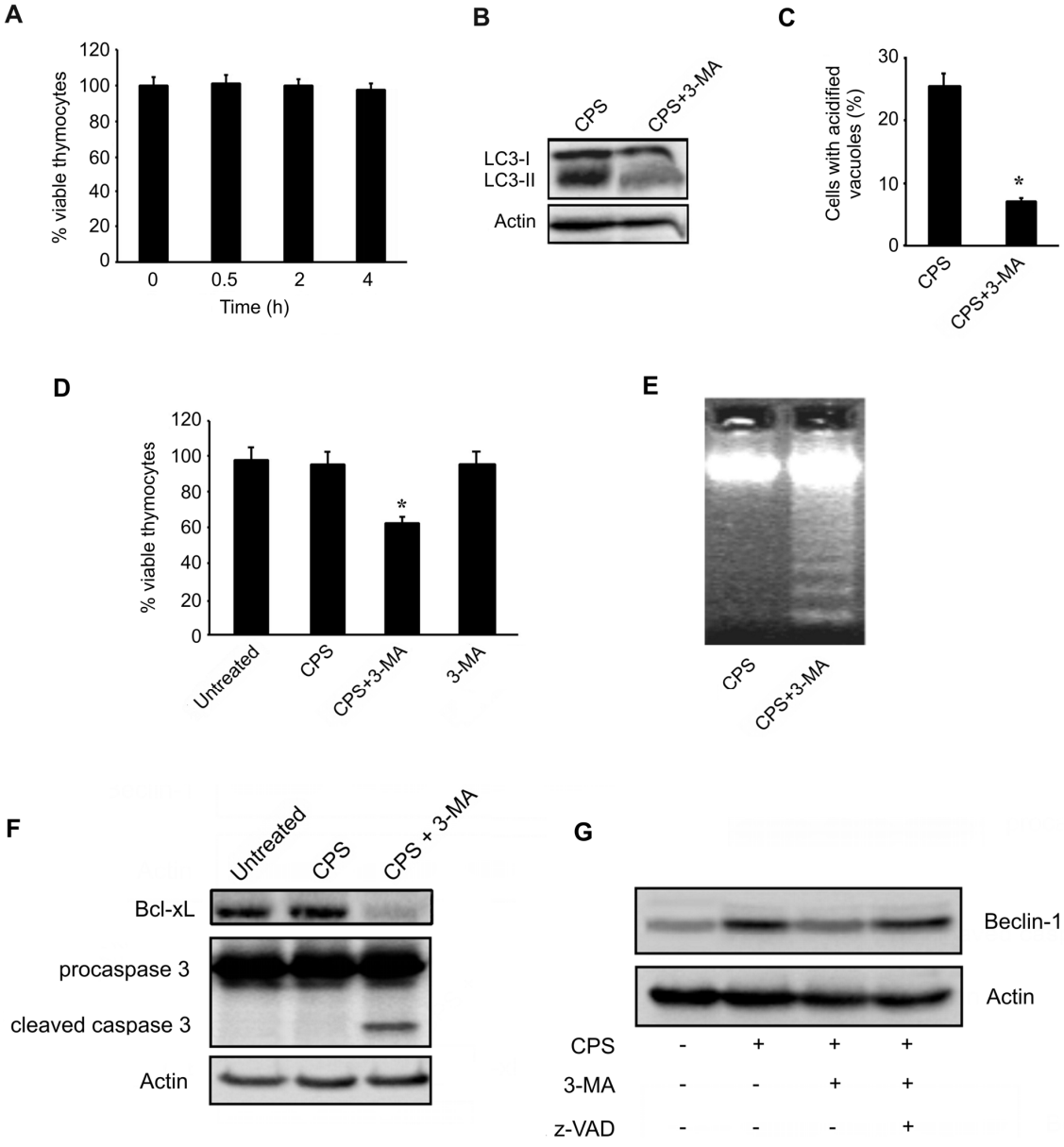


***Fig. 10 Autophagy is activated as survival pathway***

**A)** Cell viability was evaluated by Trypan Blue exclusion assay in untreated or CPS-treated thymocytes. Data shown are the mean ± SD of three independent experiments; Anova Bonferroni post-test, *p<0,01

**B)** Lysates from thymocytes treated for 2 h with CPS or pre-treated for 30 min with 3-MA before the addition of CPS, were separated on 14% SDS-PAGE and probed with anti-LC3 Ab. One representative out of three independent experiments is shown.

**C)** The percentage of cells positive for AVOs was evaluated by FACS in thymocytes treated as described in panel d. Data shown are the mean ± SD of three independent experiments; Statistical analysis was performed by comparing CPS plus 3-MA- with CPS-treated cells; Student's t-test, *p<0,01.

**D)** Cell viability was evaluated by Trypan Blue exclusion assay in thymocytes untreated, CPS- or 3MA-treated or pre-treated with 3-MA before the addition of CPS. Data shown are the mean ± SD of three independent experiments. Statistical analysis was performed by comparing CPS plus 3-MA- with CPS-treated cells or 3-MA-treated with untreated cells; Student's t-test, *p<0,01.

**E)** DNA fragmentation was assessed in thymocytes, treated as described in panel d, by agarose gel electrophoresis, ethidium bromide staining and acquisition with ChemiDoc. One representative out of three independent experiments is shown.
**F)** Lysates from thymocytes, untreated, treated for 2 h with CPS or pre-treated for 30 min with 3-MA before the addition of CPS, were separated on 14% SDS-PAGE and probed with anti-Bcl-$X_L$ and anti-caspase 3 mAbs. One representative out of three independent experiments is shown.
**G)** Lysates from thymocytes, untreated, treated for 2 h with CPS or pre-treated for 30 min with 3-MA before the addition of CPS, combined or not with z-VAD, were separated on 10% SDS-PAGE and probed with anti-Beclin-1 Ab. One representative out of three independent experiments is shown.

## 4.8 PHENOTYPE OF CPS-TREATED THYMOCYTES

To evaluate whether TRPV1 activation could affect thymocyte phenotype, we decided to analyze directly CD4 and CD8α expression on CPS-treated cells by two-colour immunofluorescence and FACS analysis. Despite no changes in main cell subset distribution were found in thymocytes treated with CPS or pre-treated with 3-MA before the addition of CPS (Table 3), the analysis of CD4 and CD8α levels in DP thymocytes showed that CPS treatment induce the development of a new DP subpopulation. Based on these observations, CPS-treated DP thymocytes (77.8% of total) can be grouped into two populations: $DP^{bright}$ (60.3%) and $DP^{dull}$ (17.5%). $DP^{bright}$ cells express CD4 and CD8α corresponding to levels seen on the majority of total DP, and $DP^{dull}$ cells have lower levels of both CD4 and CD8α. No statistically significative differences were found when comparing CPS- with CPS plus 3-MA cells (Fig. 11A, Table 3). Thereafter, we evaluated whether the $DP^{dull}$ subpopulation overlaps with the autophagic thymocytes by performing three-color FACS analysis using Abs against CD4 and CD8α in CPS-treated thymocytes from GFP-LC3 transgenic mice. By gating $DP^{bright}$ and $DP^{dull}$ thymocytes we found that all the $DP^{dull}$ cells show lower levels of LC3 green fluorescence intensity compared to $DP^{bright}$ cells (Fig. 11B), indicating that $DP^{dull}$ cells represent the thymocyte subpopulation undergoing autophagy upon CPS treatment.

Interestingly, by labelling the 3' termini of the DNA molecules with 2´-deoxyuridine, 5´-triphosphate (dUTP), we analyzed thymocytes gated from CPS- or CPS plus 3-MA-treated samples and found that $DP^{dull}$ cells show apoptotic DNA fragmentation (Fig. 11C) when autophagy is inhibited.

**Table 3. Cell subset distributions in untreated, CPS- and CPS + 3MA-treated thymocytes.**

| | **Untreated** | **CPS** | **CPS + 3-MA** |
|---|---|---|---|
| **DP** | 77.8 ± 1.6 | 77.9 ± 2.3 | 77.5 ± 1.9 |
| **$DP^{bright}$** | 69.9 ± 2.5 | 60.3 ± 3.2 | 58.7 ± 2.9 |
| **$DP^{dull}$** | 5.3 ± 0.8 | 17.5 ± 3.2* | 18.8 ± 3.4 |
| **$CD8^+$** | 5.9 ± 0.9 | 5.2 ± 1.1 | 5.4 ± 1. 0 |
| **$CD4^+$** | 11.9 ± 1.5 | 10.8 ± 1.9 | 11.3 ±1.7 |
| **DN** | 6.9 ± 0.9 | 6.1 ± 1.2 | 5.8 ± 1.1 |

Percentage of DP, $CD4^+$, $CD8^+$ and double negative (DN) subpopulations. Data shown are the mean ± SD of three independent experiments. Statistical analysis was performed comparing CPS-treated with untreated and CPS plus 3-MA with CPS-treated cells; Student's t-test.

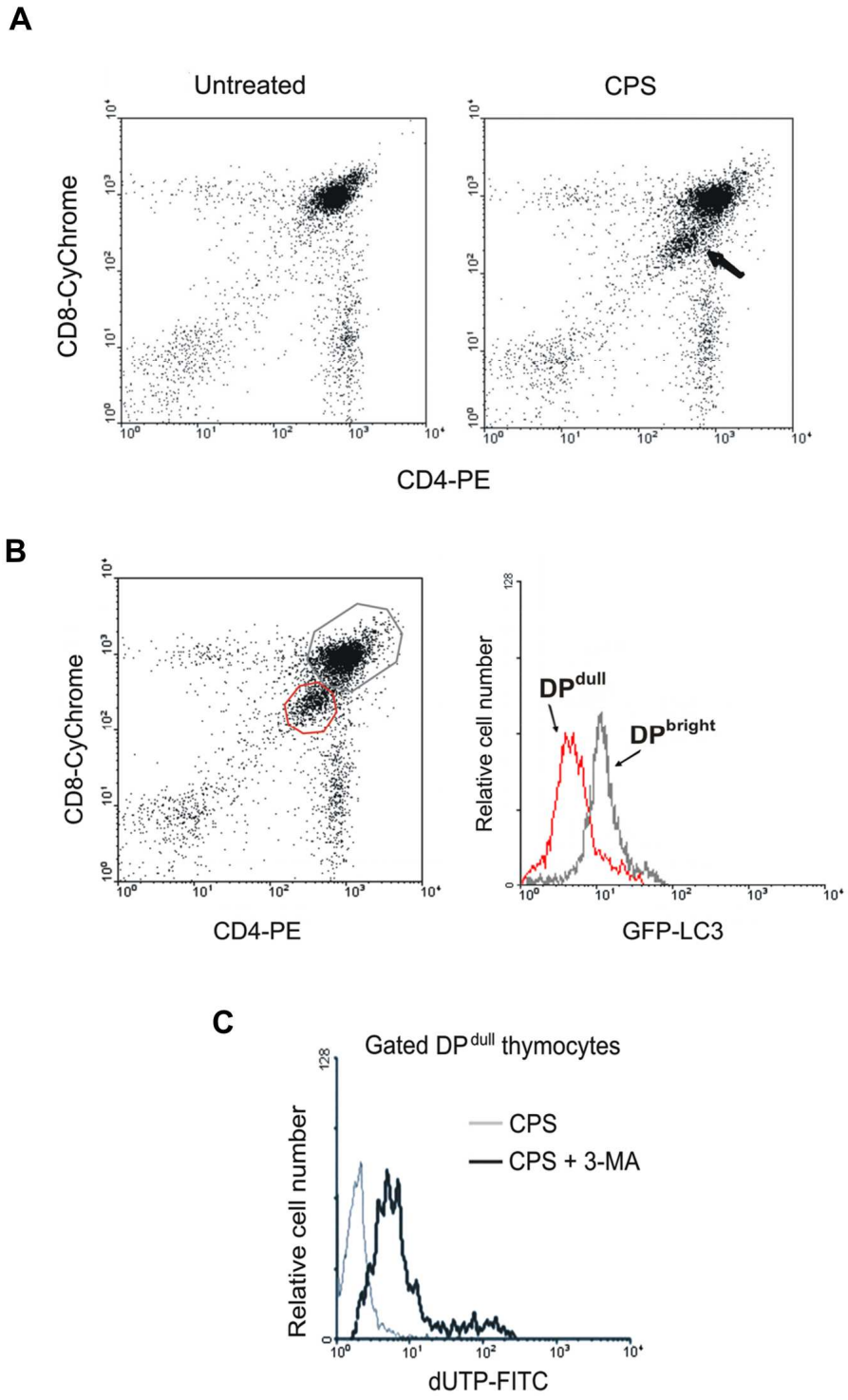


***Fig. 11 CPS treatment of thymocytes induces DP dull phenotype***

**A** Thymocytes, untreated or treated for 2 h with CPS, were stained with anti-CD4-PE and anti-CD8-CyChrome mAbs and analyzed by FACS. Arrow indicates $DP^{dull}$ subpopulation.

**B** Thymocytes from GFP-LC3 transgenic mice, treated and labeled as described in panel a, were evaluated by three color FACS analysis. LC-3 fluorescence was analyzed using separate gates for $DP^{bright}$ (R1, grey) and $DP^{dull}$ (R2, red) thymocytes.

**C** Thymocytes, treated for 2 h with CPS or pre-treated for 30 min with 3-MA before the addition of CPS, were labeled with anti-CD4-PE, anti-CD8-CyChrome and dUTP-FITC. dUTP-FITC fluorescence was analyzed by FACS in $DP^{dull}$-gated cells.
One representative out of three independent experiments is shown in each panel.

# 5. **DISCUSSION**

Autophagy has a central homeostatic role in life and death decisions of numerous cell types, functioning both as a pro-survival mechanism during nutrient deprivation and other forms of stress and as a death mechanism in other contexts [90].

Herein, we report for the first time that CPS induces TRPV1-mediated autophagy of a distinct subset of DP $^{dull}$ thymocytes in a $[Ca^{2+}]_i$- and ROS-dependent manner.

Thymocytes express TRPV1 receptor and CPS induces a TRPV1-dependent increase of $[Ca^{2+}]_i$ that is completely inhibited by EDTA and the TRPV1 antagonist, CPZ. The rise of $[Ca^{2+}]_i$ is essential for CPS-induced ROS generation and autophagy, as EDTA completely blocks CPS-induced ROS generation, LC3 lipidation and autophagy, suggesting that ROS represent a down-stream signal to $[Ca^{2+}]_i$ regulating the autophagic process. Accordingly, we found that CPS-induced ROS generation is essential for autophagy, as demonstrated by the ability of NAC to reduce the LC3 lipidation and abrogate the CPS-induced autophagy.

ROS generation induced by CPS treatment did not affect thymocyte viability, suggesting that ROS serve as signalling molecules in the autophagic pathway. Recent evidence demonstrates that AMPK activation

by calcium and ROS signaling inhibits the mTOR complex and induces autophagy [85]. We found that CPS increases the AMPK phosphorylation status in a time-dependent manner. Interestingly, thymocytes show a basal phosphorylation of AMPK, suggesting that a substantial degree of AMPK activation is required for normal energy balance. NAC and EDTA completely reverted CPS-induced AMPK phosphorylation in accordance with a role of calcium and ROS in AMPK activation [85, 91]. Moreover, the AMPK inhibitor compound C completely blocked CPS-induced autophagy, suggesting that AMPK activation is involved in thymocyte survival.

The execution of autophagy is mediated by proteins known as Atg. Atg4 is a cystein protease that cleaves LC3-I before its lipidation and association to the autophagosomal membrane. In mammals there are four assumed Atg4 paralogues (A, B, C, D) [92]. Recent reports indicate that Atg4C is not essential for autophagy development under normal conditions but is required for a proper autophagic response against stress stimuli such as prolonged starvation [93]. In this regard, we found that triggering of TRPV1 by CPS specifically increases the expression of Atg4C mRNA. Atg4s act both as conjugating and deconjugating enzymes and therefore their activity in the autophagic process is tightly regulated. Following the initial cleavage of Atg8-like proteins, Atg4 must become inactive to ensure the conjugation of Atg8/LC3 to the autophagosomal membrane [93]. ROS

have been shown to regulate starvation-induced autophagy by modulating Atg4 activity; ROS-induced oxidation causes a reversible inactivation of Atg4 and consequently the accumulation of LC3-II form [87]. In this regard, we found that CPS by stimulating ROS generation induces oxidation of Atg4C, likely promoting the LC3 lipidation, an essential step in autophagosome formation. Conversely, NAC, by blocking ROS generation, prevents Atg4C oxidation and LC3 lipidation, thus inhibiting the autophagic process.

Among the Atg proteins, Atg6/Beclin-1 was the first human protein shown to be indispensable for autophagy. Beclin-1 plays a major role in maintaining normal thymic cellularity and early B cells in the bone marrow [88]. Accordingly, we found lower levels of LC3-II in CPS-treated thymocytes from Beclin-$1^{+/-}$ mice, as compared to their wild-type counterpart, demonstrating that CPS-induced autophagy is Beclin-1-dependent.

Beclin-1 regulates autophagy in eukaryotic cells and it is ubiquitously expressed in mouse tissues [80]. We found that Beclin-1 is involved in CPS-induced autophagy of murine thymocytes and is markedly up-regulated in a TRPV1-dependent manner and in agreement with other findings [94], as a consequence of ROS production by thymocytes. More importantly, we show for the first time that Beclin-1 up-regulation is induced by AMPK activation.

Our findings also suggest the presence of a regulatory interplay between CPS-induced autophagy and apoptosis of thymocytes. CPS-induced autophagy is completely reverted by the treatment with the autophagic inhibitors that reduce cell viability and induce apoptosis of thymocytes. In addition, the exposure to 3-MA down-regulates Bcl-$X_L$, reduces the expression of Beclin-1 and induces caspase-3 activation. The pancaspase inhibitor, z-VAD, completely reverts the 3-MA-induced Beclin-1 down-regulation, indicating that Beclin-1 is cleaved after caspase activation. Finally, 3-MA down-regulates Irgm1 expression, involved in the protection of T lymphocytes from interferon gamma-induced autophagic cell death [95].

The phenotypic analysis of thymocytes evidences that CPS treatment does not influence cell distribution but affects CD4 and CD8α, but not CD3 expression, (data not shown), inducing the development of a DP subpopulation expressing lower levels of both CD4 and CD8α receptors ($DP^{dull}$). Interestingly, CPS induces autophagy only of $DP^{dull}$ thymocytes and treatment with 3-MA completely blocks CPS-mediated autophagy, and induces apoptosis of $DP^{dull}$ without affecting cell distribution. The apoptosis of $DP^{dull}$ thymocytes, in parallel with the down-regulation of Bcl-$X_L$ induced by 3-MA, is in agreement with the findings that Bcl-$X_L$ is specifically expressed in DP thymocytes and contributes to their survival [96].

The expression levels of CD4 and CD8 co-receptors are related to the thymocyte maturation phase. In TCR-transgenic mice has been demonstrated that DP thymocytes receiving either a positive or negative selection signals, can down-regulate CD4 and CD8 receptor expression before completing the differentiation to single positive cells or dying for apoptosis [97, 98]. Thus, the susceptibility of $DP^{dull}$ cells to autophagy or apoptosis strongly support the hypothesis that these cells are able to respond to either survival or death signals.

In addition our data, showing that TRPV1 activation by CPS induces ROS generation, are in accordance with previous findings demonstrating an involvement of free radicals in thymocyte development. Indeed, nitric oxide is shown to enhance the generation of $DP^{dull}$ in anti-CD3 stimulated thymocytes [99].

Overall, our results show that TRPV1-induced autophagy, via ROS-mediated Atg4C and Beclin-1 activation, could play a major role in thymocyte development. Further studies are required to investigate how autophagy participates in positive or negative selection of thymocytes.

# 6. ACKNOWLEDGEMENTS

I would like to thank Prof. Francesco Cecconi for providing GFP-LC3 and Beclin+/- transgenic mice and Prof. Giorgio Santoni for tutoring. Special thanks to Dr. Consuelo Amantini for the precious scientific support.

# 7. REFERENCES

[1] Reggiori F, Klionsky DJ (2002) Autophagy in the Eukaryotic Cell. Eukaryot Cell 1:11-21

[2] Mizushima N, Levine B, Cuervo AM, Klionsky DJ (2008) Autophagy fights disease through cellular self-digestion. Nature 451:1069-1075

[3] Schmelzle T, Hall MN (2000) TOR, a central controller of cell growth. Cell 103:253–262

[4] Abeliovich H (2004) Regulation of autophagy by the Target of Rapamycin (Tor) proteins Klionsky DJ (Ed.), Autophagy, Landes Bioscience, Georgetown, TX, 60–69

[5] Kamada Y, Funakoshi T, Sintani T, Nagano K, Ohsumi M, Ohsumi Y (2000) Tor-mediated induction of autophagy via an Apg1 protein kinase complex. J Cell Biol 150:1507–1513

[6] Codogno P, Meijer AJ (2004) Signaling pathways in mammalian autophagy. Klionsky DJ (Ed.), Autophagy, Landes Bioscience, Georgetown, TX, 26–47

[7] Petiot A, Ogier-Denis E, Blommaart EF, Meijer AJ, Codogno P (2000) Distinct classes of phosphatidylinositol 3′-kinases are involved in signaling pathways that control macroautophagy in HT-29 cells. J Biol Chem 275: 992–998

[8] Stromhaug PE, Klionsky DJ (2004) Cytoplasm to vacuole targeting. Klionsky DJ (Ed.), Autophagy, Landes Bioscience, Georgetown, TX, 84–106

[9] Kim J, Huang WP, Stromhaug PE, Klionsky DJ (2002) Convergence of multiple autophagy and cytoplasm to vacuole targeting components to a perivacuolar membrane compartment prior to de novo vesicle formation. J Biol Chem 277:763–773

[10] Suzuki K, Kirisako T, Kamada Y, Mizushima N, Noda T, Ohsumi Y (2001) The pre-autophagosomal structure organized by concerted functions of APG genes is essential for autophagosome formation. EMBO J 20:5971–5981

[11] Fengsrud M, Sneve ML, Overbye A, Seglen PO (2004) Structural aspects of mammalian autophagy. Klionsky DJ (Ed.), Autophagy, Landes Bioscience, Georgetown, TX, 11–25

[12] Kihara A, Noda T, Ishihara N, Ohsumi Y (2001) Two distinct Vps34 phosphatidylinositol 3-kinase complexes function in autophagy and carboxypeptidase Y sorting in Saccharomyces cerevisiae J Cell Biol 152:519–530

[13] Ohsumi Y (2001) Molecular dissection of autophagytwo ubiquitin-like systems. Nat Rev Mol Cell Biol 2:211–216

[14] Levine B, Klionsky DJ (2004) Development by self-digestion: molecular mechanisms and biological functions of autophagy. Dev Cell 6:463-477

[15] C.W Wang, D.J Klionsky (2003) The molecular mechanism of autophagy. Mol Med 9:65–76

[16] Zhao Z, Fux B, Goodwin M, Dunay IR, Strong D, Miller BC, Cadwell K, et al. (2008) Autophagosome-independent essential function for the

autophagy protein Atg5 in cellular immunity to intracellular pathogens. Cell Host Microbe 4:458-469

[17] Munz C (2009) Enhancing immunity through autophagy. Annu Rev Immunol 27:423-449

[18] Orvedahl A, Levine B (2009) Eating the enemy within: autophagy in infectious diseases. Cell Death Differ 16:57–69

[19] Gutierrez MG, Master SS, Singh SB, Taylor GA, Colombo MI, Deretic V (2004) Autophagy is a defense mechanism inhibiting BCG and *Mycobacterium tuberculosis* survival in infected macrophages. Cell 119:753-766

[20] Singh SB, Davis AS, Taylor GA, Deretic V (2006) Human IRGM induces autophagy to eliminate intracellular mycobacteria. Science 313:1438-1441

[21] Harris J, De Haro SA, Master SS, Keane J, Roberts EA, Delgado M, Deretic V (2007) T helper 2 cytokines inhibit autophagic control of intracellular *Mycobacterium tuberculosis*. Immunity 27:505-517

[22] Delgado M, Singh S, De Haro S, Master S, Ponpuak M, Dinkins C, Ornatowski W, et al. (2009) Autophagy and pattern recognition receptors in innate immunity. Immunol Rev 227:189–202

[23] Xu Y, Jagannath C, Liu XD, Sharafkhaneh A, Kolodziejska KE, Eissa NT (2007) Toll-like receptor 4 is a sensor for autophagy associated with innate immunity. Immunity 27:135–144.

[24] Delgado MA, Elmaoued RA, Davis AS, Kyei G, Deretic V (2008) Toll-like receptors control autophagy. EMBO J 27:1110–1121

[25] Sanjuan MA, Dillon CP, Tait SW, Moshiach S, Dorsey F, Connell S, Komatsu M, et al. (2007) Toll-like receptor signaling in macrophages links the autophagy pathway to phagocytosis. Nature 450:1253–1257

[26] Lee HK, Lund JM, Ramanathan B, Mizushima N, Iwasaki A (2007) Autophagy-dependent viral recognition by plasmacytoid dendritic cells. Science 315:1398–1401

[27] Saitoh T, Fujita N, Jang MH, Uematsu S, Yang BG, Satoh T, Omori H, et al (2008) Loss of the autophagy protein Atg16L1 enhances endotoxin-induced IL-1β production. Nature 456:264–268

[28] Jounai N, Takeshita F, Kobiyama K, Sawano A, Miyawaki A, Xin KQ, Ishii KJ, et al (2007) The Atg5 Atg12 conjugate associates with innate antiviral immune responses. Proc Natl Acad Sci USA 104:14050–14055

[29] Tal MC, Sasai M, Lee HK, Yordy B, Shadel GS, Iwasaki A (2009) Absence of autophagy results in reactive oxygen species-dependent amplification of RLR signaling. Proc Natl Acad Sci USA 106:2770–2775

[30] Cadwell K, Liu JY, Brown SL, Miyoshi H, Loh J, Lennerz JK, Kishi C, et al (2008) A key role for autophagy and the autophagy gene Atg16l1 in mouse and human intestinal Paneth cells. Nature 456:259–263

[31] Lunemann JD, Munz C (2009) Autophagy in $CD4^+$ T-cell immunity and tolerance. Cell Death Differ 16:79–86.

[32] English L, Chemali M, Duron J, Rondeau C, Laplante A, Gingras D, Alexander D, et al (2009) Autophagy enhances the presentation of endogenous viral antigens on MHC class I molecules during HSV-1 infection. Nat Immunol 10:480–487

[33] Mizushima N, Yamamoto A, Matsui M, Yoshimori T, Ohsumi Y (2004) In vivo analysis of autophagy in response to nutrient starvation using transgenic mice expressing a fluorescent autophagosome marker. Mol Biol Cell 15:1101–1111

[34] Nedjic J, Aichinger M, Emmerich J, Mizushima N, Klein L (2008) Autophagy in thymic epithelium shapes the T-cell repertoire and is essential for tolerance. Nature 455:396–400

[35] Virgin HW, Levine B (2009) Autophagy genes in immunity. Nat Immunol 10:461-70

[36] Arsov I, Li X, Matthews G, Coradin J, Hartmann B, Simon AK, Sealfon SC, Yue Z (2008) BAC-mediated transgenic expression of fluorescent autophagic protein Beclin 1 reveals a role for Beclin 1 in lymphocyte development. Cell Death Differ 15:1385–1395

[37] Stephenson LM, Miller BC, Ng A, Eisenberg J, Zhao Z, Cadwell K, Graham DB, et al (2009) Identification of *Atg5*-dependent transcriptional changes and increases in mitochondrial mass in *Atg5*-deficient T lymphocytes. Autophagy 5:625-35

[38] Pua HH, Dzhagalov I, Chuck M, Mizushima N, He YW (2007) A critical role for the autophagy gene Atg5 in T cell survival and proliferation. J Exp Med 204:25–31

[39] Pua HH, Guo J, Komatsu M, He YW (2009) Autophagy is essential for mitochondrial clearance in mature T lymphocytes. J Immunol 182:4046–4055

[40] Miller BC, Zhao Z, Stephenson LM, Cadwell K, Pua HH, Lee HK, Mizushima NN, et al (2007) The autophagy gene ATG5 plays an essential role in B lymphocyte development. Autophagy 4:309–314

[41] Mellen MA, de la Rosa EJ, Boya P (2008) The autophagic machinery is necessary for removal of cell corpses from the developing retinal neuroepithelium. Cell Death Differ 15:1279–1290

[42] Feng CG, Zheng L, Jankovic D, Báfica A, Cannons JL, Watford WT, Chaussabel D, et al (2008) The immunity-related GTPase Irgm1 promotes the expansion of activated CD4+ T cell populations by preventing interferon-γ-induced cell death. Nat Immunol 9:1279-1287

[43] Li C, Capan E, Zhao Y, Zhao J, Stolz D, Watkins SC, Jin S, Lu B (2006) Autophagy is induced in $CD4^+$ T cells and important for the growth factor-withdrawal cell death. J Immunol 177:5163–5168

[44] Espert L, Denizot M, Grimaldi M, Robert-Hebmann V, Gay B, Varbanov M, Codogno P, Biard-Piechaczyk M (2006) Autophagy is involved in T cell death after binding of HIV-1 envelope proteins to CXCR4. J Clin Invest 116:2161–2172

[45] Clapham DE (2003) TRP channels as cellular sensors. Nature 426:517-524

[46] Niemeyer BA (2005) Structure-function analysis of TRPV channels. Naunyn Schmiedebergs Arch Pharmacol 371:285-294

[47] Kahn-Kirby AH, Bargmann CI (2006) TRP channels in C. elegans. Annu Rev Physiol 68:719-736

[48] Clapham DE, Runnels LW, Strübing C (2001) The TRP ion channel family. Nat Rev Neurosci 2:387-396

[49] den Dekker E, Hoenderop JG, Nilius B, Bindels RJ (2003) The epithelial calcium channels, TRPV5 & TRPV6: from identification towards regulation. Cell Calcium 33:497-507

[50] Kedei N, Szabo T, Lile JD, Treanor JJ, Olah Z, Iadarola MJ, Blumberg PM (2001) Analysis of the native quaternary structure of vanilloid receptor 1. J Biol Chem 276:28613-28619

[51] Amiri H, Schultz G, Schaefer M (2003) FRET-based analysis of TRPC subunit stoichiometry. Cell Calcium 33:463-470

[52] Schaefer M (2005) Homo- and heteromeric assembly of TRP channel subunits. Pflugers Arch 451:35-42

[53] Zagranichnaya TK, Wu X, Villereal ML (2005) Endogenous TRPC1, TRPC3, and TRPC7 proteins combine to form native store-operated channels in HEK-293 cells. J Biol Chem 280:29559-29569

[54] Pedersen SF, Owsianik G, Nilius B (2005) TRP channels: an overview. Cell Calcium 38:233-252

[55] Caterina MJ, Schumacher MA, Tominaga M, Rosen TA, Levine JD, Julius D (1997) The capsaicin receptor: a heatactivated ion channel in the pain pathway. Nature 389:816–824

[56] Sedgwick SG, Smerdon SJ (1999) The ankyrin repeat: a diversity of interactions on a common structural framework. Trends Biochem Sci 24:311–316

[57] Rosenbaum T, Gordon-Shaag A, Munari M, Gordon SE (2004) CaCa2+/calmodulin modulates TRPV1 activation by capsaicin. J Gen Physiol 123:53–62

[58] Harteneck C (2003) Proteins modulating TRP channel function. Cell Calcium 33:303–310

[59] Kedei N, Szabo T, Lile JD, Treanor JJ, Olah Z, Iadarola MJ, Blumberg PM (2001) Analysis of the native quaternary structure of vanilloid receptor 1. J Biol Chem 276:28613-28619

[60] Kuzhikandathil EV, Wang H, Szabo T, Morozova N, Blumberg PM, Oxford GS (2001) Functional analysis of capsaicin receptor (vanilloid

receptor subtype 1) multimerization and agonist responsiveness using a dominant negative mutation. J Neurosci 21:8697–8706

[61] Smith GD, Gunthorpe MJ, Kelsell RE, Hayes PD, Reilly P, Facer P, Wright JE, Jerman JC, Walhin JP, Ooi L, Egerton J, Charles KJ, Smart D, Randall AD, Anand P, Davis JB (2002) TRPV3 is a temperature-sensitive vanilloid receptor-like protein. Nature 418:186-190

[62] Gunthorpe MJ, Harries MH, Prinjha RK, Davis JB, Randall A (2000) Voltage- and time-dependent properties of the recombinant rat vanilloid receptor (rVR1). J Physiol (Lond) 525:747-759

[63] Liu L, Wang Y, Simon SA (1996) Capsaicin activated currents in rat dorsal root ganglion cells. Pain 64:191-195

[64] Premkumar LS, Agarwal S, Steffen D (2002) Single-channel properties of native and cloned rat vanilloid receptors. J Physiol (Lond) 545:107-117

[65] Tominaga M, Caterina MJ, Malmberg AB, Rosen TA, Gilbert H, Skinner K, Raumann BE, Basbaum AI, Julius D (1998) The cloned capsaicin receptor integrates multiple pain-producing stimuli. Neuron 21:531-543

[66] Vriens J, Appendino G, Nilius B (2009) Pharmacology of vanilloid transient receptor potential cation channels. Mol Pharmacol 75:1262-1279

[67] Nilius B, Owsianik G, Voets T, Peters JA (2007) Transient Receptor Potential Cation Channels In Disease. Physiol Rev 87:165–217

[68] Gallo EM, Cante-Barrett K, Crabtree GR (2006) Lymphocyte calcium signaling from membrane to nucleus. Nat Immunol 7:25–32

[69] Dolmetsch RE, Lewis RS, Goodnow CC, Healy JI (1997) Differential activation of transcription factors induced by Ca2+ response amplitude and duration. Nature 386:855–858

[70] Panyi G, Varga Z, Gaspar R (2004) Ion channels and lymphocyte activation. Immunol Lett 92:55–66

[71] Mori Y, Wakamori M, Miyakawa T, Hermosura M, Hara Y, Nishida M, Hirose K, et al (2002) Transient receptor potential 1 regulates capacitative Ca2+ entry and Ca2+ release from endoplasmic reticulum in B lymphocytes. J Exp Med 195:673–681

[72] Launay P, Cheng H, Srivatsan S, Penner R, Fleig A, Kinet JP (2004) TRPM4 regulates calcium oscillations after T cell activation. Science 306:1374–1377

[73] Lievremont JP, Numaga T, Vazquez G, Lemonnier L, Hara Y, Mori E, Trebak M, et al. (2005) The role of canonical transient receptor potential 7 in B-cell receptor-activated channels. J Biol Chem 280:35346–35351

[74] Jin J, Desai BN, Navarro B, Donovan A, Andrews NC, Clapham DE (2008) Deletion of Trpm7 disrupts embryonic development and thymopoiesis without altering Mg2+ homeostasis. Science 322:756-760.

[75] Juzan M, Hostein I, Gualde N (1992) Role of thymus-eicosanoids in the immune response. Prostaglandins Leukot Essent Fatty Acids 46:247-255.

[76] Amantini C, Mosca M, Lucciarini R, Perfumi M, Morrone S, Piccoli M, Santoni G (2004) Distinct thymocyte subsets express the vanilloid receptor VR1 that mediates capsaicin-induced apoptotic cell death. Cell Death Differ 11:1342-1356.

[77] Yue Z, Jin S, Yang C, Levine AJ, Heintz N (2003) Beclin 1, an autophagy gene essential for early embryonic development, is a haploinsufficient tumor suppressor. Proc Natl Acad Sci USA 100:15077–15082.

[78] Shvets E, Elazar Z (2009) Flow cytometric analysis of autophagy in living mammalian cells. Methods Enzymol 452:131-141.

[79] Graf MR, Jia W, Johnson RS, Dent P, Mitchell C, Loria RM (2009) Autophagy and the functional roles of Atg5 and beclin-1 in the anti-tumor effects of 3beta androstene 17alpha diol neuro-steroid on malignant glioma cells. J Steroid Biochem Mol Biol 115:137-145

[80] Arsov I, Li X, Matthews G, Coradin J, Hartmann B, Simon AK, Sealfon SC, Yue Z (2008) BAC-mediated transgenic expression of fluorescent autophagic protein Beclin 1 reveals a role for Beclin 1 in lymphocyte development. Cell Death Differ 15:1385-1395.

[81] Nedjic J, Aichinger M, Emmerich J, Mizushima N, Klein L (2008) Autophagy in thymic epithelium shapes the T-cell repertoire and is essential for tolerance. Nature 455:396-400.

[82] Hail N Jr (2003) Mechanisms of vanilloid-induced apoptosis. Apoptosis 8:251-262

[83] Ravikumar B, Sarkar S, Davies JE, Futter M, Garcia-Arencibia M, Green-Thompson ZW, Jimenez-Sanchez M et al (2010) Regulation of mammalian autophagy in physiology and pathophysiology. Physiol Rev 90:1383-1435.

[84] Wang C, Hu HZ., Colton CK, Wood JD, Zhu MX (2004) An alternative splicing product of the murine trpv1 gene dominant negatively modulates the activity of TRPV1 channels. J Biol Chem 279:37423-37430.

[85] Prasad A, Bloom MS, Carpenter DO (2010) Role of calcium and ROS in cell death induced by polyunsaturated fatty acids in murine thymocytes. Cell Physiol 225:829-836.

[86] Alexander A, Cai SL, Kim J, Nanez A, Sahin M, MacLean KH, Inoki K, Guan KL, Shen J, Person MD, Kusewitt D, Mills GB, Kastan MB, Walker CL (2010) ATM signals to TSC2 in the cytoplasm to regulate mTORC1 in response to ROS. Proc Natl Acad Sci USA 107:4153-4158.

[87] Sanz P (2008) AMP-activated protein kinase: structure and regulation. Curr Protein Pept Sci 9:478-492.

[88] Scherz-Shouval R, Shvets E, Fass E, Shorer H, Gil L, Elazar Z (2007) Reactive oxygen species are essential for autophagy and specifically regulate the activity of Atg4. EMBO J 26:1749-1760.

[89] Arsov I, Adebayo A, Kucerova-Levisohn M, Haye J, MacNeil M, Papavasiliou FN, Yue Z, Ortiz BD (2011) A role for autophagic protein beclin 1 early in lymphocyte development. J Immunol 186:2201-2209.

[90]. Furuya N, Liang XH, Levine B (2004) Autophagy and cancer. In: Klionsky DJ (ed) Autophagy, Landes Bioscience, Georgetown, pp 241-255.

[91] Høyer-Hansen M, Bastholm L, Szyniarowski P, Campanella M, Szabadkai G, Farkas T, Bianchi K Fehrenbacher N, Elling F, Rizzuto R, Mathiasen IS, Jäättelä M (2007) Control of macroautophagy by calcium, calmodulin-dependent kinase kinase-beta, and Bcl-2. Mol. Cell. 25:193-205.

[92] Mariño G, Uría JA, Puente XS, Quesada V, Bordallo J, López-Otín C (2003) Human autophagins, a family of cysteine proteinases potentially implicated in cell degradation by autophagy. J Biol Chem 278:3671-3678.

[93] Mariño G, Salvador-Montoliu N, Fueyo A, Knecht E, Mizushima N, López-Otín C (2007) Tissue-specific autophagy alterations and increased tumorigenesis in mice deficient in Atg4C/autophagin-3. J Biol Chem 282:18573-18583.

[94] Djavaheri-Mergny M, Amelotti M, Mathieu J, Besançon F, Bauvy C, Souquère S, Pierron G, Codogno P (2006) NF-kappaB activation represses tumor necrosis factor-alpha-induced autophagy. J Biol Chem 281:30373-30382.

[95] Feng CG, Zheng L, Lenardo MJ, Sher A (2009) Interferon-inducible immunity-related GTPase Irgm1 regulates IFN gamma-dependent host defense, lymphocyte survival and autophagy. Autophagy 5:232-234.

[96] Ma A, Pena JC, Chang B, Margosian E, Davidson L, Alt FW, Thompson CB (1995) Bcl-XL regulates the survival of double-positive thymocytes. Proc Natl Acad Sci USA 92:4763-4767.

[97] Kersh GJ, Hedrick SM (1995) Role of TCR specificity in CD4 versus CD8 lineage commitment. J Immunol 154:1057-1068.

[98] McGargill MA, Hogquist KA (1999) Antigen-induced coreceptor down-regulation on thymocytes is not a result of apoptosis. J Immunol 162:1237-1245.

[99] Tai XG, Toyo-oka K, Yamamoto N, Yashiro Y, Mu J, Hamaoka T, Fujiwara H (1997) Expression of an inducible type of nitric oxide (NO) synthase in the thymus and involvement of NO in deletion of TCR-stimulated double-positive thymocytes. J Immunol 158:4696